RETAIN ALL WORK UNTIL AFTER PUBLICATION OF FINAL RESULTS
DEPARTMENT OF MECHANICAL ENGINEERING
ASSESSMENT COVER SHEET

Family Name: JOSEPH	First Name: ADRIEL SEBASTIAN
Student ID: 30061636	
Unit Code & Name: MEC 3458: Experimental Project	
Name of assessment task: Research Final Report	
Name of Lecturers: *Dr. Foo Ji Jinn*	
Tutorial Day & Time: Fri 9am-12pm & 3pm - 6pm	Group No: 10
Due Date: 9/112020	Date submitted: 9/11/2020

All work must be submitted by the due date. If an extension of work is granted this must be specified with the signature of the lecturer/tutor.

Extension granted until (date) ....… Signature of lecturer/tutor………………...

MONASH University

DEPARTMENT OF MECHANICAL ENGINEERING

ASSESSMENT COVER SHEET

Family Name: LIM	First Name: WEI CHUN
Student ID: 30061636	

Unit Code & Name:	
MEC 3458: Experimental Project	
Name of assessment task:	
Research Final Report	
Name of Lecturers: *Dr. Foo Ji Jinn*	

Tutorial Day & Time: Fri 9am-12pm & 3pm - 6pm	Group No: 10
Due Date: 9/11/2020	Date submitted: 9/11/2020

All work must be submitted by the due date. If an extension of work is granted this must be specified with the signature of the lecturer/tutor.

Extension granted until (date) ....… Signature of lecturer/tutor………………...

MONASH University

DEPARTMENT OF MECHANICAL ENGINEERING

ASSESSMENT COVER SHEET

Family Name: TOH	First Name: WU PENG
Student ID: 29825040	
Unit Code & Name: MEC 3458: Experimental Project	
Name of assessment task: Research Final Report	
Name of Lecturers: *Dr. Foo Ji Jinn*	
Tutorial Day & Time: Fri 9am-12pm & 3pm - 6pm	**Group No: 10**
Due Date: 9/11/2020	**Date submitted: 9/11/2020**

All work must be submitted by the due date. If an extension of work is granted this must be specified with the signature of the lecturer/tutor.

Extension granted until (date) ....… Signature of lecturer/tutor………………...

MONASH University

Family Name: YONG	First Name: WEN JUN
Student ID: 30099412	

Unit Code & Name:
MEC 3458: Experimental Project

Name of assessment task:
Research Final Report

Name of Lecturers: *Dr. Foo Ji Jinn*

Tutorial Day & Time: Fri 9am-12pm & 3pm - 6pm	Group No: 10
Due Date: 9/11/2020	**Date submitted: 9/11/2020**

All work must be submitted by the due date. If an extension of work is granted this must be specified with the signature of the lecturer/tutor.

Extension granted until (date) ....… Signature of lecturer/tutor………………...

MONASH University

ASSESSMENT COVER SHEET

Family Name: OOI	**First Name: JIA YONG**
Student ID: 28902092	

Unit Code & Name:
MEC 3458: Experimental Project

Name of assessment task:
Research Final Report

Name of Lecturers: *Dr. Foo Ji Jinn*

Tutorial Day & Time: Fri 9am-12pm & 3pm - 6pm	**Group No: 10**
Due Date: 9/11/2020	**Date submitted: 9/11/2020**

All work must be submitted by the due date. If an extension of work is granted this must be specified with the signature of the lecturer/tutor.

Extension granted until (date) ....… Signature of lecturer/tutor………………...

Please note that it is your responsibility to retain copies of your assignments before submitting.
Plagiarism and Collusion are methods of cheating for the purposes of Monash Statute 4.2 -Discipline
Plagiarism
Plagiarism is the presentation of work which has been copied in whole or in part from another person's work, or from any other source such as the Internet, published books or periodicals without due acknowledgment given in the text.
**Collusion**
Collusion is the presentation of work which is the result in whole or in part of unauthorised collaboration with another person or persons.
Where there are reasonable grounds for believing that cheating has occurred, the only action that may be taken when plagiarism or collusion is detected is for the staff member not to mark the item of work and to report or refer the matter to the Dean. This may result in work being disallowed and given a fail grade or if the circumstances warrant, the matter may be referred to a Committee of Inquiry for investigation. Such investigation may result in the matter being referred to the University Discipline Committee which has the power to exclude a student.
Student's statement:
I certify that I have not plagiarised the work of others or participated in unauthorised collusion when preparing this assignment.
                                      Signature: ....
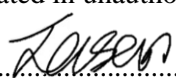
MONASH University

DEPARTMENT OF MECHANICAL ENGINEERING
ASSESSMENT COVER SHEET

Family Name: ARNAUT	First Name: ABDULHADI FAIZ
Student ID: 29825040	
Unit Code & Name: MEC 3458: Experimental Project	
Name of assessment task: Research Final Report	
Name of Lecturers: *Dr. Foo Ji Jinn*	
Tutorial Day & Time: Fri 9am-12pm & 3pm - 6pm	Group No: 10
Due Date: 9/11/2020	Date submitted: 9/11/2020

All work must be submitted by the due date. If an extension of work is granted this must be specified with the signature of the lecturer/tutor.

Extension granted until (date) ....… Signature of lecturer/tutor………………..·

MEC3458 Research Report

Experimental based numerical validation on SSG 0.2 – induced turbulence

Supervisor: Dr. Foo Ji Jinn

Group 10, 2020

Student ID	First Name	Last Name
30236843	JOSEPH	ADRIEL SEBASTIAN
30061636	WEI CHUN	LIM
29825040	TOH	WU PENG
30099412	YONG	WEN JUN
28902092	OOI	JIA YONG
28272514	ARNAUT	ABDULHADI FAIZ

RESEARCH TITLE: EXPERIMENTAL BASED NUMERICAL VALIDATION ON SSG 0.2 – INDUCED TURBULENCE

W.C.LIM (30061636,10), A.S. JOSEPH (30236843,10), W.P.TOH (29825040,10), W.J. YONG (30099412,10), J.Y.OOI (28902092,10), and A.F. ARNAUT (28272514,10)

MEC3458, Department of Mechanical Engineering

Monash University, Clayton, Victoria, 3800 AUSTRALIA

ABSTRACT

This paper presents the experimental based numerical validation of single square grid induced turbulence. The turbulence modelling is done by the linear pressure-strain Reynolds Stress Model (RSM) with ANSYS Fluent ver19.2. There are 9 constant parameters associated with the model which their values are manipulated explicitly to best replicate the experimental results conducted by Laizet et al. Mesh convergence test is carried out to ensure that all the parameter changes will be independent to the mesh quality. A mesh size of 18mm is found to be the most suitable one because the trend and shape of the graph is the smoothest and closest to the experimental data. Among the 9 parameters tested, the two dissipation parameters, $C_{1,\epsilon}$ and $C_{2,\epsilon}$, are found to have huge influence on the turbulence intensity curve. This is due to the presence of single square grid which facilitates the dissipation rate of the flow and the details are explained in the discussion presented. Furthermore, it is observed that $C_{1,\epsilon}$ has slightly more impact than $C_{2,\epsilon}$ in the tuning process. Hence, it can be concluded that $C_{1,\epsilon}$ is the most dominant parameter in turbulence modelling followed by $C_{2,\epsilon}$. The optimum value for $C_{1,\epsilon}$ is discovered to be around 1.581 with a percentage error of 0.15% whereas for $C_{2,\epsilon}$ is around 1.718 with a percentage error of 0.06%. However, all 9 parameters are found to have no effect in shifting the velocity profile of the induced turbulence. This paper also presents some suggestions on how to improve the simulation results in the future.

INTRODUCTION

Turbulent flow is a form of flow in fluids, during which the fluid particles undergo mixing, sudden changes in direction, irregular and often chaotic fluctuations. This is a large contrast to laminar flow where the fluid flows in a smooth, predictable and orderly manner. During turbulent flow of a fluid, each particle is undergoing a change in speed, direction and magnitude. Due to this behaviour of particles during turbulent flow, turbulent flow plays a key role in enchantment of fluid mixing, increased heat transfer rate (Due to the particles colliding and exchanging heat energy), and momentum transfer [1]. The phenomenon just described is named as "Turbulent diffusion" in the academic community. Turbulent diffusion has been studied by famous researchers for generations and it is known to occur when a turbulent system reaches critical conditions in a response to shear flow, which then results in the formation and combination of steep concentration gradients, density gradients and high relative velocities [1]. Turbulence diffusion has been extensively used in industrial applications such as in stir tank reactors and plug and flow reactors.

When a fluid flows past an object that has not been streamlined (Such objects are sometimes called "Bluff Bodies"), such as a cube, at certain velocities, an oscillating pattern in the flow will be observed. This phenomenon is known as "Vortex Shedding". During Vortex shedding, vortices are formed behind the body and will detach themselves periodically from either side of the body. This results in alternating low-pressure areas which in turn results the creation of additional vortices further downstream.

One of the methods used to trigger turbulence is by having a grid on the surface area of an enclosed pipe or duct thus creating an external force to distort the fluid flow. In the enclosed channel, vortex shedding is created as the fluid flows past the grid thus also forming eddies. This type of grid-generated turbulence is normally done in a rectangular bar using a space-filling fractal square grid. According to I.Paul,G.Papadakis and J.C.Vassilicos in 2017, the turbulence flow generated by the grid has two regions, the first region is nearest to the grid where the intensity of the turbulence is at the peak. The second region is the immediate adjacent downstream region where the turbulence decay. Initially, the flow along the grid element centreline is non-turbulent but soon it transfers to become turbulent due to the infiltration of turbulent wakes from the grid element bars. The generated turbulence from the grid is often homogeneous with isotropic small [2].
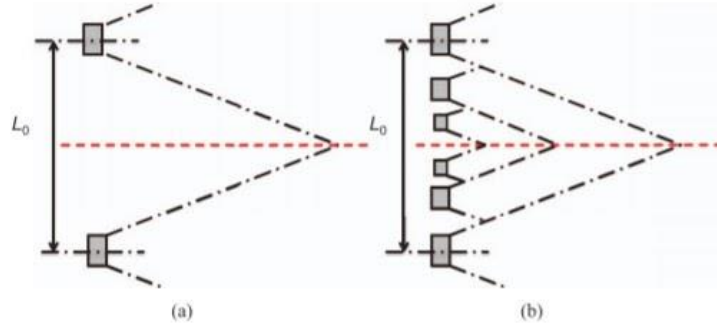
Figure 1 shows the schematics of wake interactions following Mazellier and Vassilicos [4][6],
(a) Single square grid and (b) fractal square grid

With reference to Figure 1, it shows the schematic wake interaction of two types of grid-generated turbulence as the fluid flow passes through the grid and further into the closed-rectangular channel. The turbulence which has been generated can be assumed to be always homogeneous with small isotropic characteristics [2]. In our research, we are using a single square grid with the blockage ratio of 0.20 to induce the turbulence. This ratio is achieved by changing the dimensions of the grid. The single-square grid is located at the inlet of the channel to create a force from outside to distort the fluid flow. As the fluid passes through the grid, vortex shedding is created and also the formations of the eddies behind the grid in enclosed channels. According to Zhou et al [3], single square grid is one of the types of the regular or classical grid which only allow the research to understand the behaviour of the turbulence generated by that specific grid only when using a large mesh meaning to say by having a large regular bar. A very specific conjecture has also been made by Mazellieer and Vassilicos [4], that only simulation by using a large mesh size can determine the interaction of wake further from the centreline of the rectangular bar. From the conjecture, a formula can be proposed for the wake interaction length x^*:

$$x^* = \frac{L_o{}^2}{t_o}$$

(1)

[L_o is the length of the largest mesh size and t_o is the thickness of the largest mesh size]

From the similar conjecture, Mazellieer and Vassilicos [4] has made experimental report that the turbulence intensity at X_{peak} is equal to $0.45x^*$. From this experimental report, it can be concluded that the value of X_{peak} is totally dependent on the mesh size. Thus, it is not wrong if the value gotten from the current single square grid to have a turbulent profile indistinguishable to the experimental data from the single square grid because the turbulent profile is mainly dependent on the size of the mesh and independent of the Reynolds number Re and the pattern of the grid.

In the fundamental research, special properties of turbulent flow which makes it a highly complicated process is when it's three-dimensional, non-linear, being diffusive, with large Reynolds number and having irregularity in time and space. In the same vein, Argyr-opoulos and Markatos in 2015 has stated that modelling with turbulent flow is the best way to go because it saves a considerable amount of money by removing the need for prototyping, changing technology to provide improved turbulence understanding and also for experimentation [5].

After years of research, it is proven that the fractal square grid is better to be implemented in generating turbulent flow than the single square grid. The fractal grids can be categorized to I-grid, cross-grid and square grid which is used and compared predominantly with the other class of grids [6]. The main reason for using this fractal grid-generated turbulence it has a very high intensity which can be extended to several distances with a small pressure drop [7]. Plus, a fractal square grid also has a better mixing performance compared to a single square grid. However, it is also proven that a single square grid produces turbulence intensity and turbulent Reynolds number until the end of the simulation region compared to the higher-blockage fractal square grid [3]. Furthermore, it was also proven that the peak velocity is almost entirely dependent on the blockage ratio of the single square grid. By using a blockage ratio of 0.11 (which is 0.9 lesser than our blockage ratio), it is proven that the acceleration is 20 % lesser. As for the turbulence intensity, it increases in the production region and reaches the peak. The flow then experiences a decay region where the U_{rms} start to decrease. Another research also shows that the single square grid with a larger L_o or t_o and with a low blockage ratio can produce a higher turbulent intensity and heat transfer compared to other types of grid [6]. This research proves that both types of

the turbulent flow have unique energy decay rates. Although many engineering sectors are using the applications of the turbulent flow to run the process, some literature review revealed that the 100% understanding behind the theory and physics of turbulent flow is yet to be obtained. Thus, these imperfections give motivation to conduct this research proposal with induced turbulence using the single square grid which can benefit some engineering applications in near future.

The research based on the fluid dynamics of the turbulent flow is highly crucial and plays an important role in scientific research because it has a powerful influence in improving the fluid flow, fluid pressure, thermal energy generated in the fluid and also the momentum transfer in the flow. Therefore, Computational Fluid Dynamics (CFD) will be used in our research to study the turbulent flow generated by the single square grid. The use of CFD has made a huge contribution to today's engineering world because CFD can simulate the Navier-Stokes Equation. Thus, the fluid dynamics of the turbulent flow can be studied very well and be used to improve the industries which are related. The Navier-Stoke equation can be used to determine the velocity of the flow and also can be used to visualize the behaviour of the fluid at that moment. At the same time, it consumes a lot of time in the process plus the cost is very high to perform. Plus, the graph also produces fluctuations due to the non-linearity in the equation. Thus, Reynolds average Navier-Stokes equation (RANS) could be the best replacement to the Navier-Stokes Equation because it represents every turbulent flow as $U = \bar{U} + U'$, $\bar{U}$ is the mean value and U' is fluctuating value [8]. Reynolds Stress Model (RSM) is one of the key turbulent models from the RANS which is most commonly used to solve the problems.

Direct numerical simulation (DNS) is one of the most powerful implements for the further study of the turbulent flow in three dimensions. Spectral method and finite difference are the commonly categorized numerical methods of the DNS. Both types of the numerical methods have their own pros and cons. Spectral method is highly accurate compared to the finite difference method, but its function and application is limited. Finite difference can be less accurate buthen it can be used for complex geometry. The finite difference method can achieve the accuracy as the spectral method by improving the fully conservative higher order finite difference scheme in the immersed boundary method [9]. Thus, by this improvement, a finite difference scheme could be the best choice. By further proceeding into the investigation on the extensive experiments and direct numerical simulations (DNS) carried out on the turbulence generated by the fractal square grid, can come to the conclusion on how the 8 important parameters can cause the turbulent flow. These parameters have been the key for the direct numerical simulation (DNS) to determine the location of highest turbulence intensity distribution which can also be tuned by varying the function of the important parameters. These different scales of the geometry parameters can give a unique turbulent flow that has been induced by the fractal grids compared to the uniform grid. By changing the scales of the geometry, the direct numerical scale (DNS) allow the interaction of these scales and exhibits a very unique property of the flow which can be regarded as "New Class of Turbulence" [6]. As the assumption made primarily, DNS also shows that the fractal grid produces the smallest wake interaction nearest to the grid and largest wake furthest from the grid [6][10][11].

Although direct numerical simulations (DNS) is very accurate, it then needs a high cost to perform this application. Plus DNS is not adequate to perform complex geometry for example like the fractal grid with large Re [9][10]. Therefore, in our research we are using a software called ANSYS Fluent to study the turbulent flow by manipulating the mesh size for the already manipulated values of the 8 geometry parameters. From this manipulation, the ANSYS Fluent software can be used to generate two graphs which are Velocity Peak vs streamwise coordinate graph and Turbulent Intensity versus streamwise coordinate graph.

This report is divided into multiple sections. In the Methods section, a detailed overview of the steps undertaken to conduct this research using the Reynolds Stress Model (RSM) in ANSYS Fluent are outlined. In the results section, the data from the research are tabulated and generated two graphs (Velocity Peak graph and Turbulent Intensity graph) using Microsoft Excel for each of the manipulated geometrical parameters from these findings. The result section is later discussed in the discussion section. Finally, about the conclusion about the whole experiment.

METHODS

Introduction

The simulation of turbulence flow for single square grid (SSG) was done using Ansys Fluent. Ansys Fluent was chosen due to it being able to provide usage of many turbulence models. The Reynolds Stress Model (RSM)

used in the project is one of the many Reynolds Averaged Navier Stokes (RANS) based models. It requires relatively high computational power but is considered as the most physically sound RANS model in Ansys Fluent. Additionally, RSM is recommended for complex and high swirling flows which would prove beneficial for this project.

Modelling

The single square grid (SSG) has a width of 229mm denoted as L_o, thickness of 43mm denoted as t_o and thickness of 6mm in the streamwise direction. These dimensions were given as recommendations from the following research paper [2].
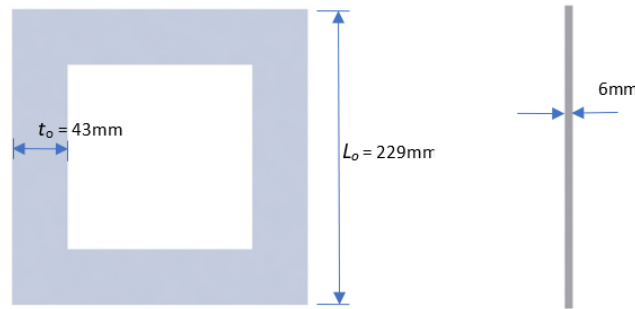

Figure 2: Schematic illustrating the dimensions of SSG

The SSG was positioned in the center of the channel and the inlet area of the channel was modelled so that a blockage ratio of 0.2 was achieved. The distance from the inlet to the SSG was modelled as $1.75L_o$ and the characteristic wake interaction length denoted as x^*, was calculated by using the formula $x^* = \frac{L_o^2}{t_o}$.
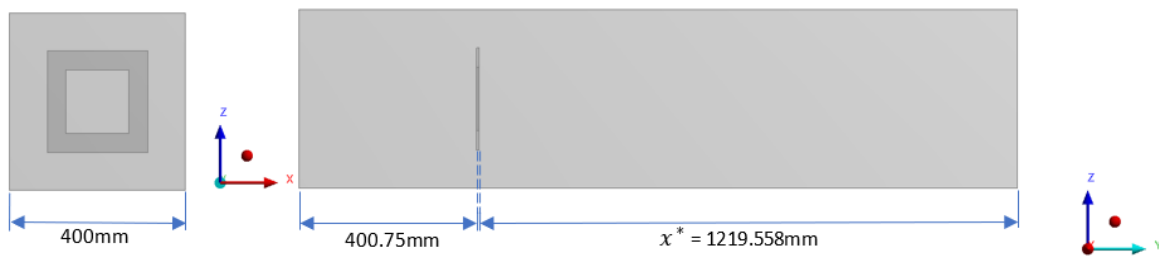

Figure 3: Schematic illustrating the position of SSG in the channel

The Single Square Grid (SSG) and the channel were designed via SolidWorks separately. Both CAD files were then saved as Initial Graphics Exchange Specification (IGES) file and imported to DesignModeller under ANSYS Workbench. Boolean operations were then used to segregate the SSG from the channel. Under Boolean operations type, the "subtract" option was chosen. This is necessary as Ansys Fluent will assign the SSG as liquid by default. By doing this step, the SSG was set as solid while the channel was set as liquid where the analysis would be based on.

Meshing

Once DesignModeler was set up, the model was meshed in the meshing section found in the Ansys Workbench window. All settings in meshing were made default except for the element size. The element size was varied between 16mm to 23mm. 16mm element size gave the highest mesh number possible of 490,000 for ANSYS Fluent Academic License. On the other hand, 23mm element size gave the lowest acceptable mesh number of 200,000. The inlet, outlet and wall of the channel were also labelled during meshing using the "name selection" function. By doing this, Ansys will automatically register these names as actual Inlets, Outlets and Walls, allowing a variety of changes to be made for both in the simulation section.
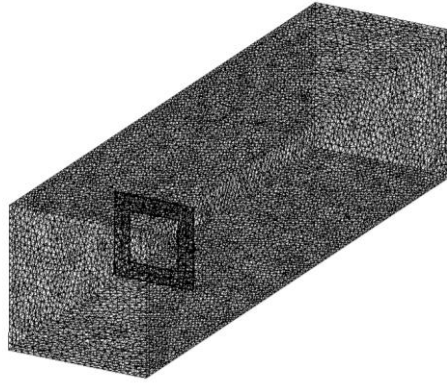
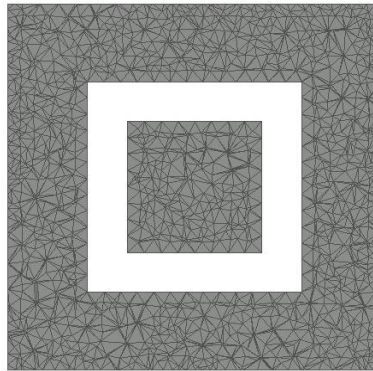*Figure 4: Isometric view of 18mm element size mesh of simulated model*

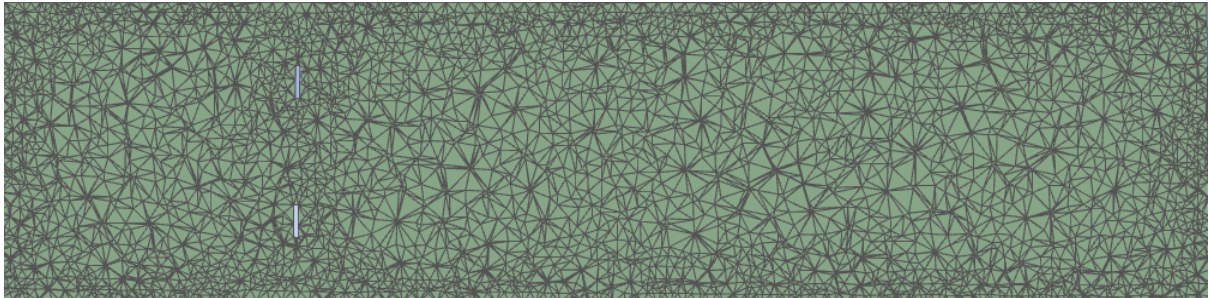*Figure 5: Image of mesh of SSG positioned at the center of the channel*

Figure 6: Image showing the streamwise mesh view of the channel

The variation of element sizes was to conduct the mesh convergence test. The test was conducted for each parameter change as well as the default parameters, resulting in 3 sets of data for each unique parameter change and default parameters. In total, 10 sets of graphs were generated, each illustrating the velocity ratio and turbulent intensity graphs. Complete results of the mesh independence test can be found in the results section.

Setup of the numerical simulation

For the solver in general setup, the time calculation of the solver needs to be in steady state and gravity of 9.81m/s² was enabled. The Linear pressure-strain Reynolds stress model was chosen as the viscous model. All the initial parameters in the viscous model remain unchanged to produce a default graph of streamwise evolution of normalized mean velocity and turbulence intensity along the centerline of the square grid. This default graph is known as the benchmark for each parameter variation estimation. Under boundary condition of the inlet zone, the free-stream and constant velocity magnitude, U_{in} is 2.5m/s as low inlet velocity will create laminar flow before the flow passes through the single square grid to reduce the chances of the turbulence flow formation caused by the inlet velocity. For the specification method of the turbulence in the velocity inlet, a value of 0% of turbulence intensity and 0.628952m hydraulic diameter was used. Other than that, the Reynolds number of fluid flow is approximately 5000 with the unchanged value of the fluid properties. SIMPLEC algorithm is applied under the solution of method as it can discretize the computation domain with a

standard pressure and First Order Upwind discretization of RSM. The hybrid initialization is used to run the simulation. After the initialization, turbulence intensity needs to be selected under the data file quantities before the simulation starts as it is not a common quantity under ANSYS FLUENT software.

The model selected is a linear pressure-strain Reynolds stress model which was suggested by Gibson and Launder[12], Fuetal,[13] and Launder[14,15]. The transport equation of Reynolds stresses in RSM modelling is shown in figure [7]. The default parameters value are $C_\mu = 0.09, C_{1,\epsilon} = 1.44, C_{2,\epsilon} = 1.92, C_{1-PS} = 1.8, C_{2-PS} = 0.6, C'_{1-PS} = 0.5, C'_{2-PS} = 0.3, Pr_{TKE} = 1$ and $Pr_{TDR} = 1.3$.The simulation was set to run for 50000 iterations, however it converged at much smaller iterations (about 300-2000 iterations).

$$\underbrace{\frac{\partial}{\partial t}(\rho \overline{u_i' u_j'})}_{\text{Local Time Derivative}} + \underbrace{\frac{\partial}{\partial x_k}(\rho u_k \overline{u_i' u_j'})}_{C_{ij} \equiv \text{Convection}} = \underbrace{-\frac{\partial}{\partial x_k}\left[\rho \overline{u_i' u_j' u_k'} + \overline{p(\delta_{kj} u_i' + \delta_{ik} u_j')}\right]}_{D_{T,ij} \equiv \text{Turbulent Diffusion}} + \underbrace{\frac{\partial}{\partial x_k}\left[\mu \frac{\partial}{\partial x_k}(\overline{u_i' u_j'})\right]}_{D_{L,ij} \equiv \text{Molecular Diffusion}}$$

$$- \underbrace{\rho\left(\overline{u_i' u_k'}\frac{\partial u_j}{\partial x_k} + \overline{u_i' u_k'}\frac{\partial u_i}{\partial x_k}\right)}_{P_{ij} \equiv \text{Stress Production}} \quad \underbrace{\rho\beta(g_i \overline{u_j'\theta} + g_j \overline{u_i'\theta})}_{G_{ij} \equiv \text{Buoyancy Production}}$$

$$+ \underbrace{\overline{p\left(\frac{\partial u_i'}{\partial x_j} + \frac{\partial u_j'}{\partial x_i}\right)}}_{\varphi_{ij} \equiv \text{Pressure Strain}} - \underbrace{2\mu \overline{\frac{\partial u_i'}{\partial x_k}\frac{\partial u_j'}{\partial x_k}}}_{\varepsilon_{ij} \equiv \text{Dissipation}} - \underbrace{2\rho\Omega_k(\overline{u_j' u_m'}\varepsilon_{ikm} + \overline{u_i' u_m'}\varepsilon_{jkm})}_{F_{ij} \equiv \text{Production by System Rotation}}$$

$$+ \underbrace{S_{user}}_{\text{User-Defined Source Term}}$$

Figure 7: Transport equation of Reynolds stress in RSM Modelling

Post-processing

After the simulation data of the default parameters for the model has been obtained, the parameters in Linear pressure-strain Reynolds stress model were varied one by one to find the dominant parameters that would fit the simulation data obtained by Zhou et al. The experimental data from Laizer et al was extracted by using the online tool named "Web Plot Digitizer" which was used to extract the numerical data from plots in the image format and detect the axis resolution. A centre line was drawn from the single square grid to the end of the characteristic wake interaction length scale in the Post-processing workbench section and 500 points were extracted from this center line. The extracted velocity and turbulence intensity data from ANSYS fluent was saved in the CSV file format and Microsoft excel was introduced to plot the results obtained. All the simulation data that were obtained from ANSYS FLUENT were given one parameter change at an instant while the other parameters remained constant. The velocity ratio and turbulent intensity at a particular point of x/x^* for all the changes for a particular parameter was plotted. A best fit line was then drawn on the plotted data. The effect of each parameter was then observed by comparing the gradient of the fitted lines of each parameter to find the dominant parameter for both velocity ratio and turbulent intensity.

Results
Experimental data

Velocity Peak		Turbulence Intensity	
x/x^*	U/U_∞	x/x^*	U_{rms}/U
0	1.36867325	0.01049848	0.00153866
0.10534299	1.55908989	0.11704308	0.03284513
0.19796393	1.25835189	0.29609709	0.09796728
0.29942924	1.19465604	0.41069273	0.13354570
0.39441879	1.16083038	0.49967352	0.14170085
0.50906899	1.12280422	0.59849019	0.13880648
0.60569206	1.08684914	0.70542333	0.13412703
0.70070494	1.06156449	0.79618893	0.12696071
0.79737469	1.04269143	0.90153722	0.11907531
0.90063688	1.03665322		
0.99567893	1.02204483		

Table 1: Experimental data based on $U_\infty = 2.5 m/s$ obtained by extracting the data points from the Laizet et al.
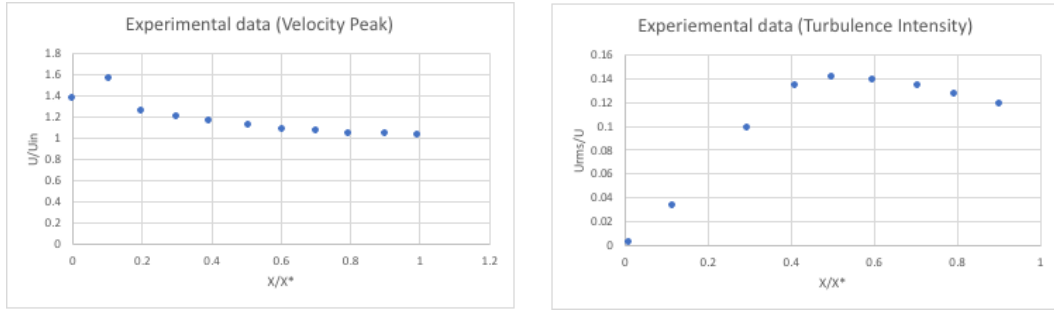
Figure 8: Plotted graph of the experimental data

Mesh Convergence Test

Mesh convergence test will be carried for all the parameter changes. This is to ensure that all the parameter changes will be independent to the mesh quality. Therefore, mesh sizes ranging from 18mm to 23mm are tested in default parameters and also in various parameter changes which includes: $C_\mu = 0.06, C_{1,\epsilon} = 1.55, C_{2,\epsilon} = 1.74, C_{1-PS} = 2.8, C_{2-PS} = 0.4, C'_{1-PS} = 0.25, C'_{2-PS} = 0.1, Pr_{TKE} = 0.8$ and $Pr_{TDR} = 1.0$.

Throughout the changes, the results show that the graph data are consistent and so the mesh convergence test has almost achieve the ideal result. However, no clear conclusion to keep reducing the mesh size as the results will still deviate and a high computation cost is needed for mesh size that is lower than 18mm. Besides that, it is found that the higher the mesh size, the higher the frequency of fluctuation has. Therefore, a mesh size of 18mm will be the most suitable mesh size to be carried out throughout the experiment. This is because the trend and shape of the graph is the smoothest and closest to the experimental data among the tests. Besides, the mesh size of 18mm will have around 490,000 number of elements.
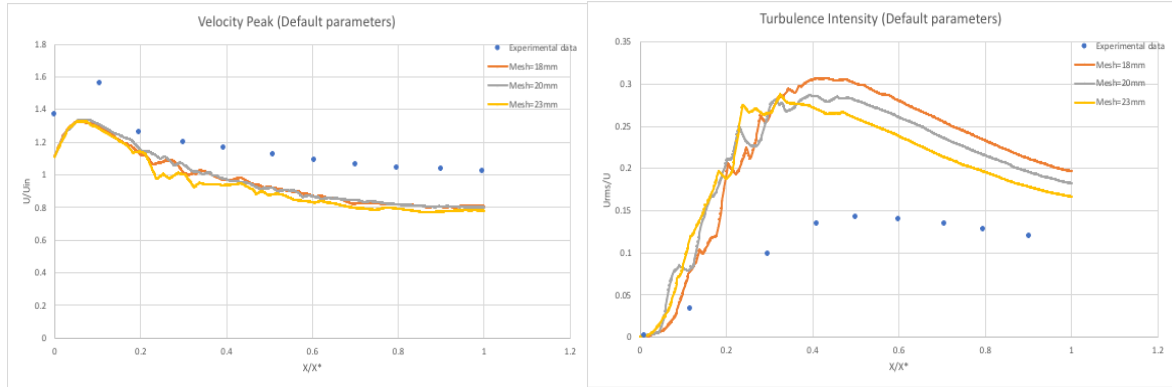
Default Parameters

Figure 9: Default Velocity Peak and Turbulence Intensity Mesh Convergence Test graph
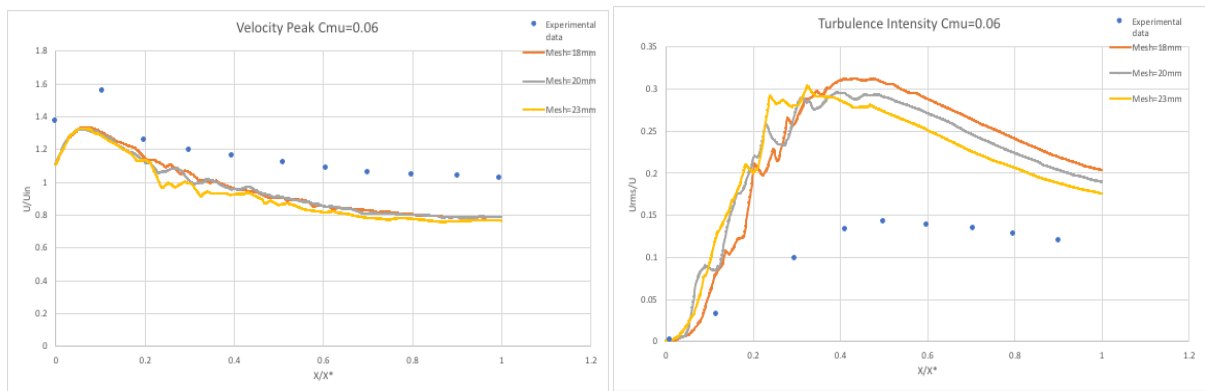
$C_\mu = 0.06$

Figure 10: $C_\mu = 0.06$ Velocity Peak and turbulence Intensity Mesh Convergence Test graph
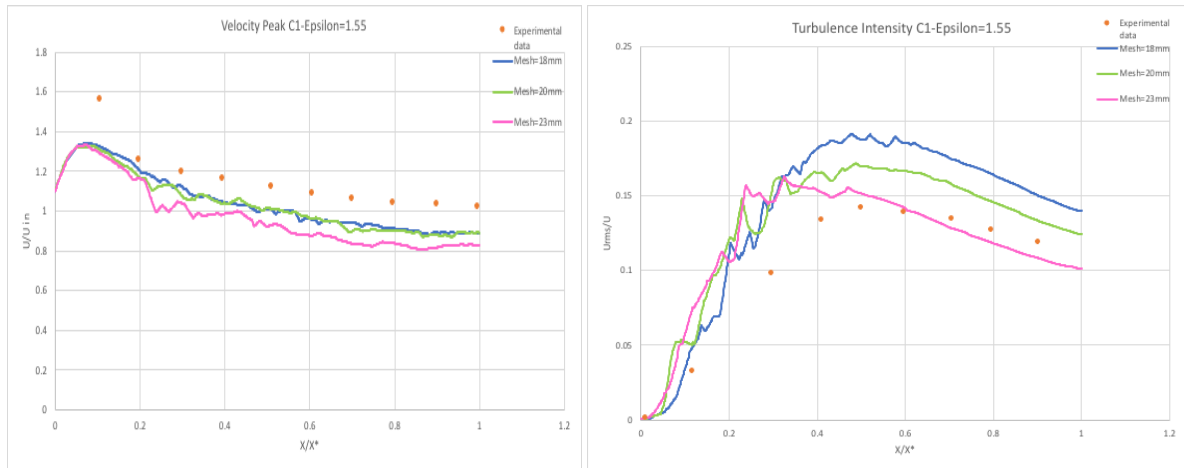
$C_{1,\epsilon} = 1.55$

Figure 11: $C_{1,\epsilon} = 1.55$ Velocity Peak and Turbulence Intensity Mesh Convergence Test graph
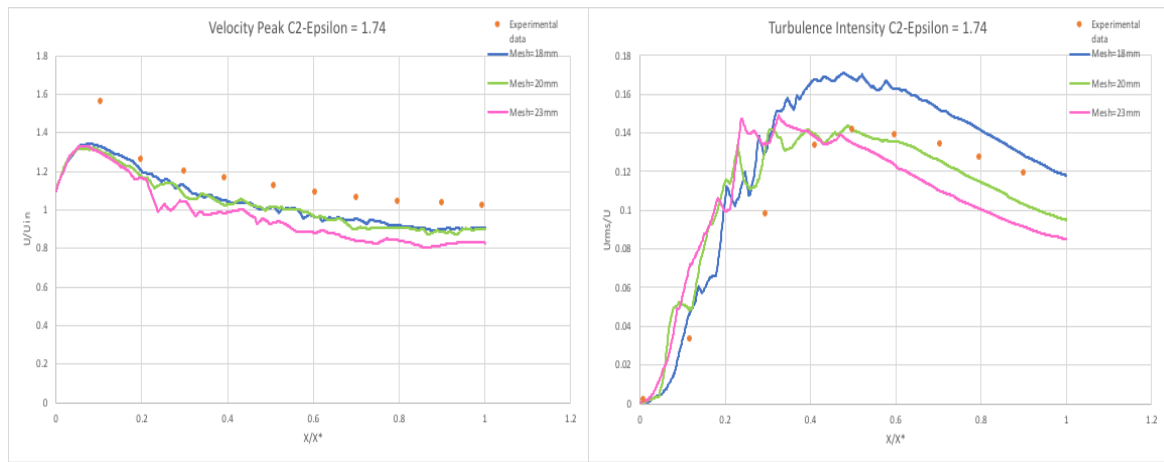
$C_{2,\epsilon} = 1.74$

Figure 12: $C_{2,\epsilon} = 1.74$ Velocity Peak and Turbulence Intensity Mesh Convergence Test graph
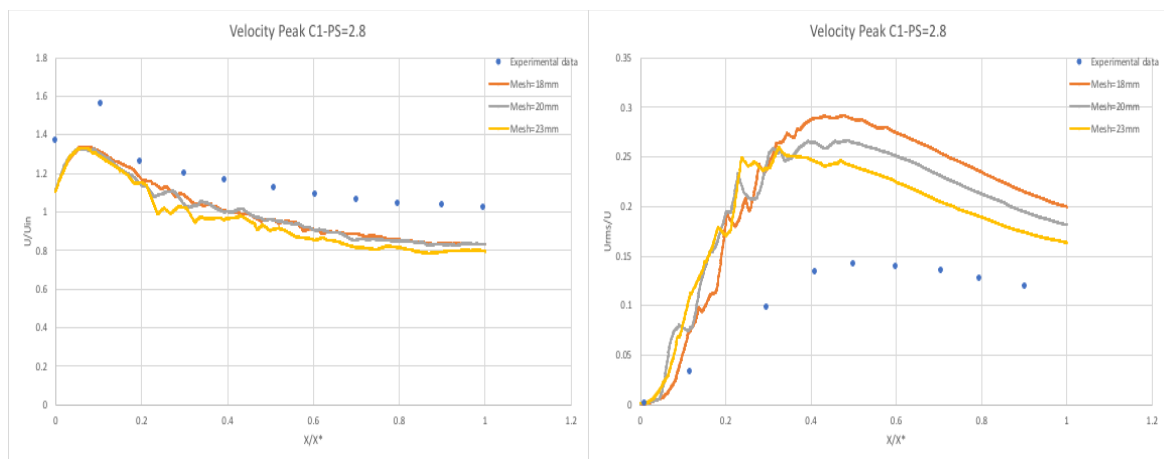
$C_{1-PS} = 2.8$

Figure 13: $C_{1-PS} = 2.8$ Velocity Peak and Turbulence Intensity Mesh Convergence Test graph
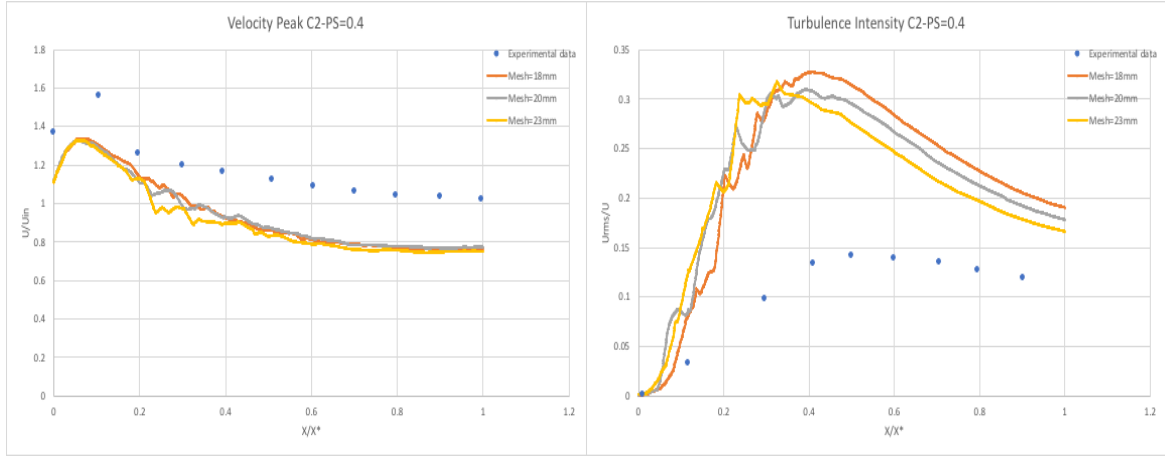
$C_{2-PS} = 0.4$

Figure 14: $C_{2-PS} = 0.4$ Velocity Peak and Turbulence Intensity Mesh Convergence Test graph

$C'_{1-PS} = 0.25$

Figure 15: $C'_{1-PS} = 0.25$ Velocity Peak and Turbulence Intensity Mesh Convergence Test graph

$C'_{2-PS} = 0.1$
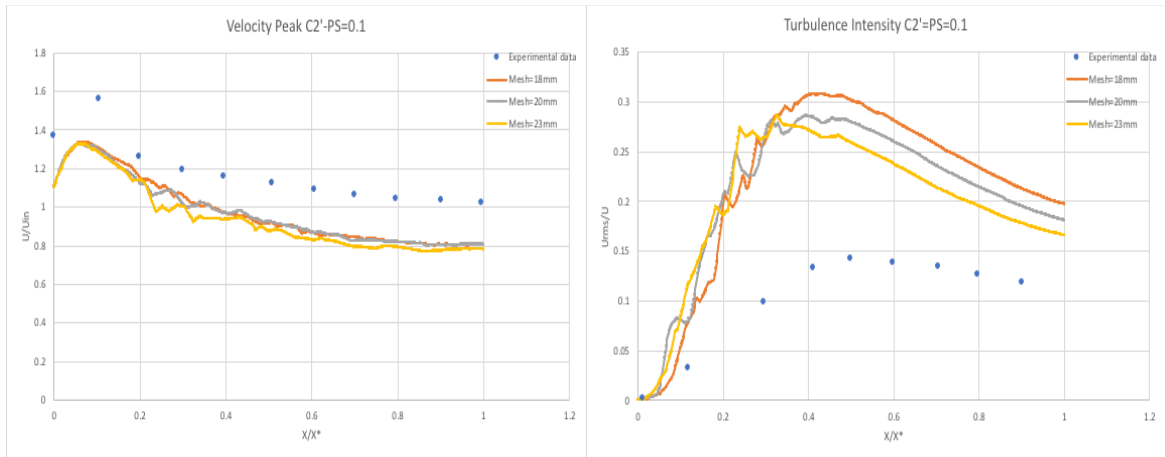
Figure 16: $C'_{2-PS} = 0.1$ Velocity Peak and Turbulence Intensity Mesh Convergence Test graph

$Pr_{TKE} = 0.8$
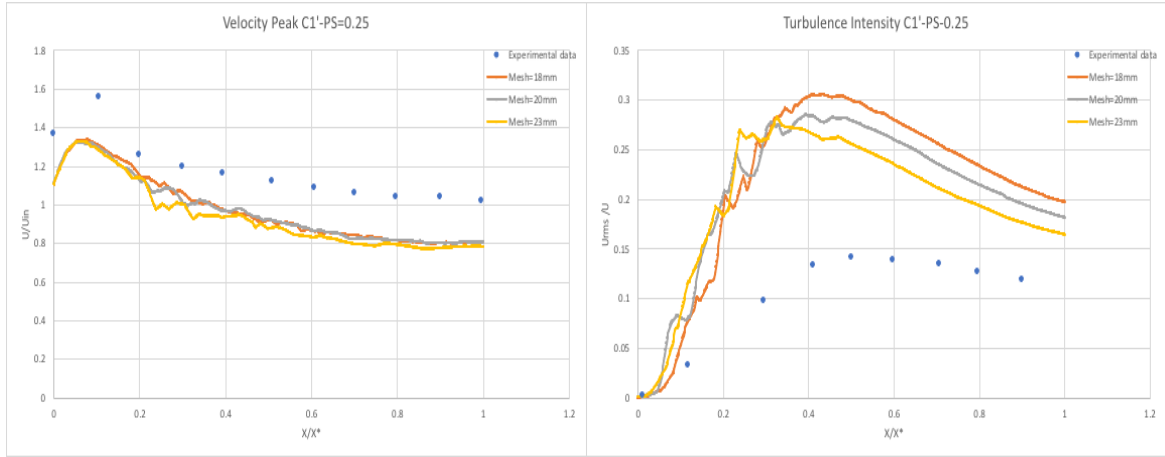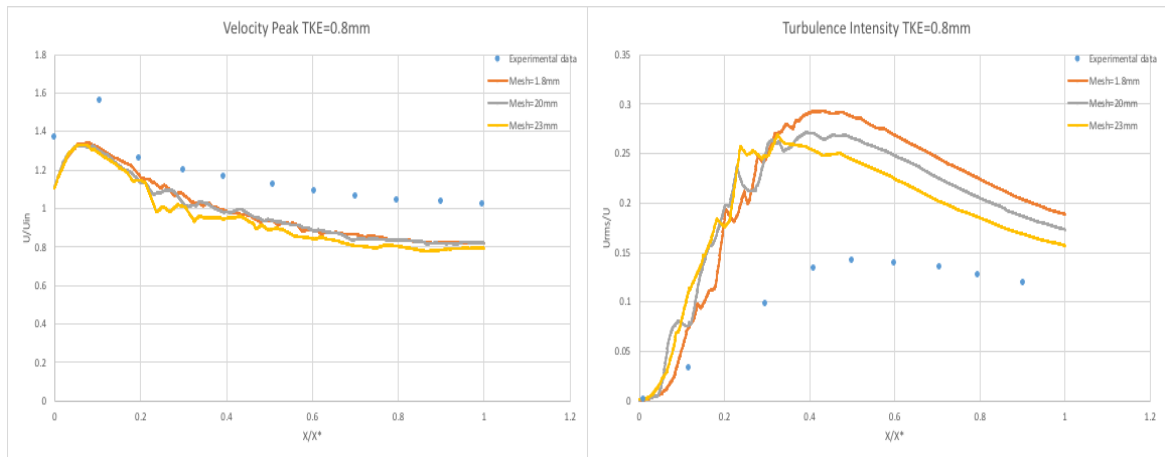

Figure 17: $Pr_{TKE} = 0.8$ Velocity Peak and Turbulence Intensity Mesh Convergence Test graph

$Pr_{TDR} = 1.0$
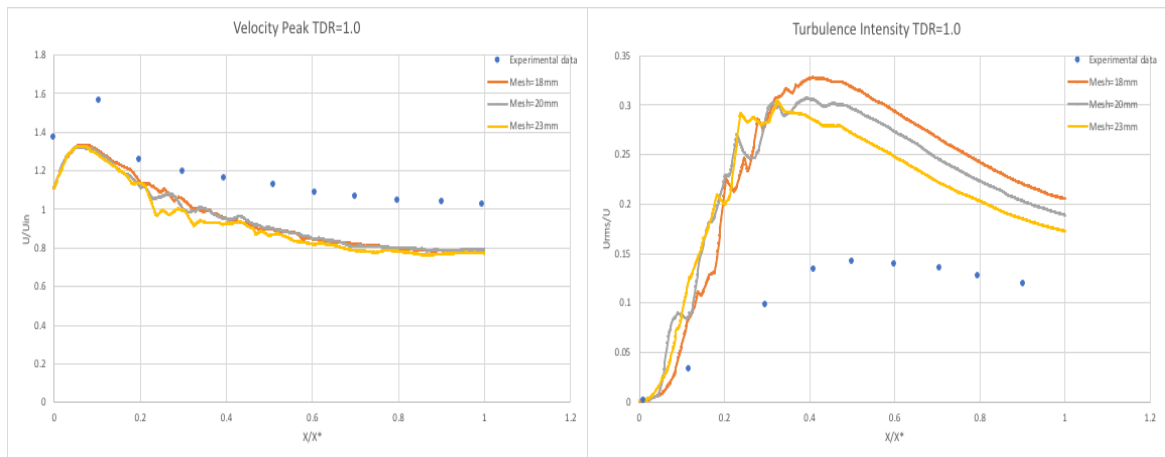
Figure 18: $Pr_{TDR} = 1.0$ Velocity Peak and Turbulence Intensity Mesh Convergence Test graph

Parameter Variation

1st Parameter: C_μ
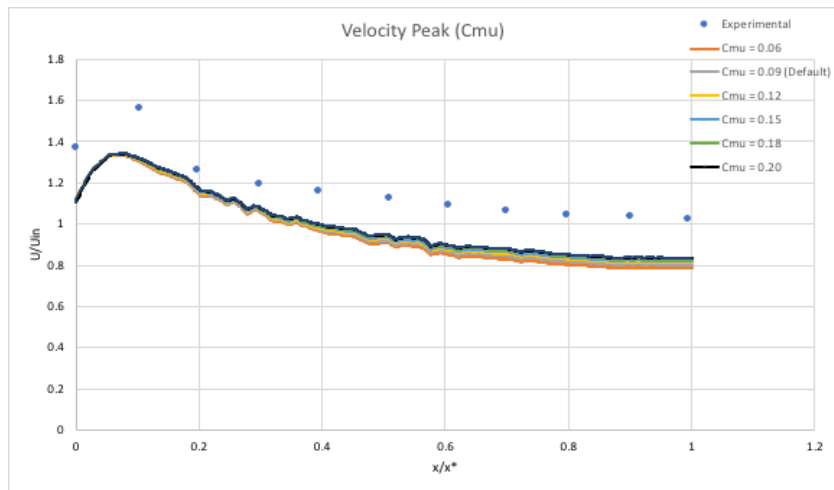
Figure 19: C_μ Velocity Peak graph
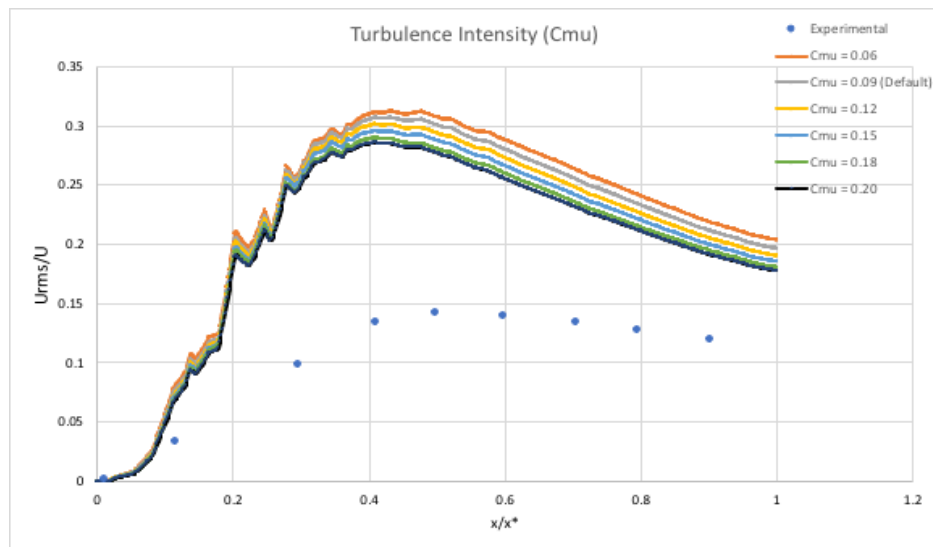
Figure 20: C_μ Turbulence Intensity graph
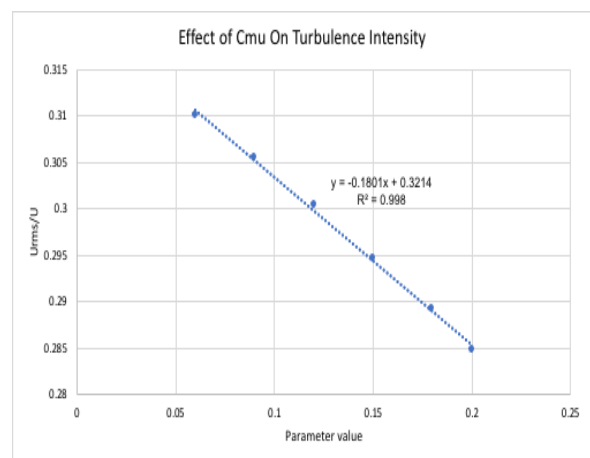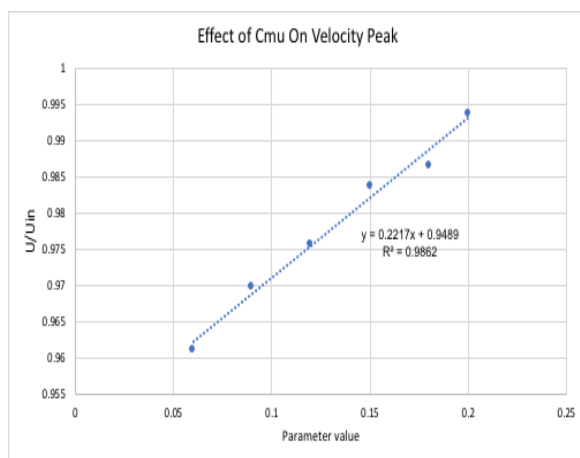
Figure 21: Effect of C_μ On Velocity Peak and Turbulence Intensity graph

2nd Parameter: C$_{1,\epsilon}$
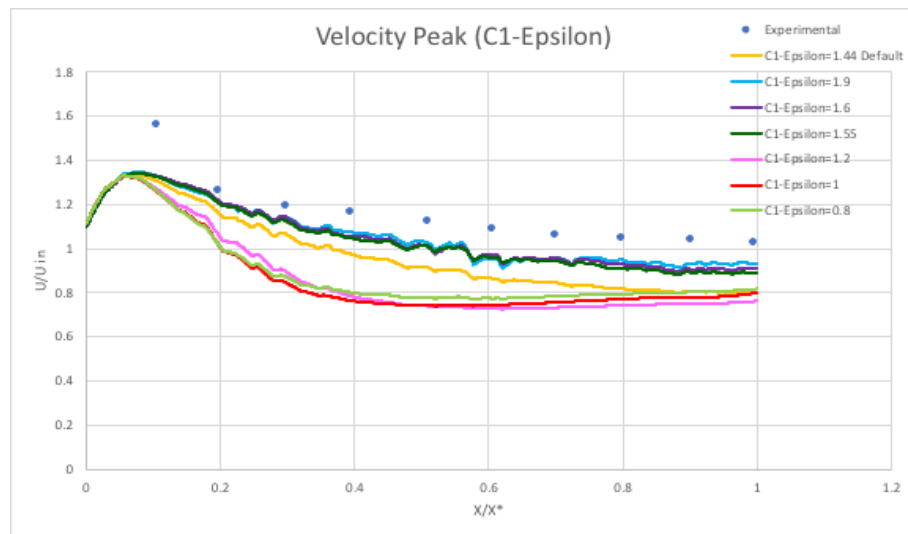
Figure 22: $C_{1,\epsilon}$ Velocity Peak graph
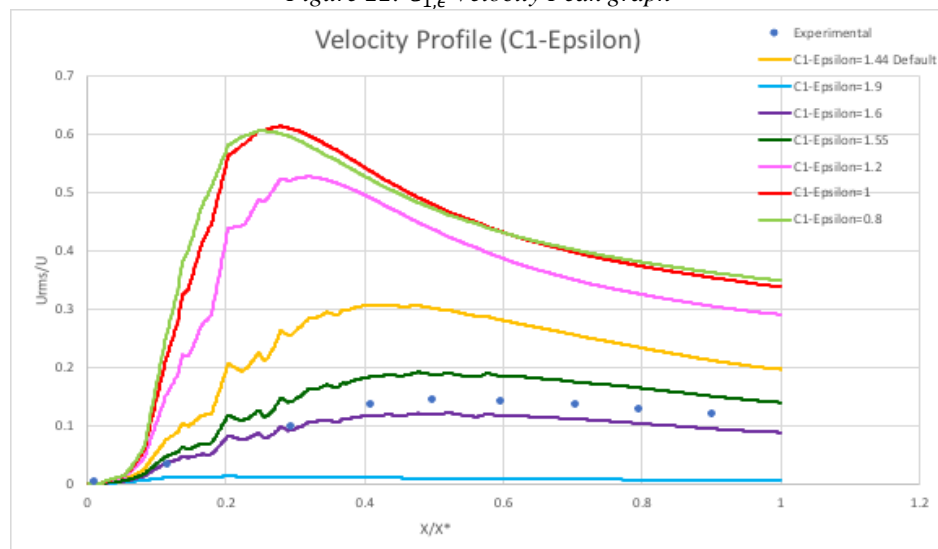
Figure 23: $C_{1,\epsilon}$ Turbulence Intensity graph
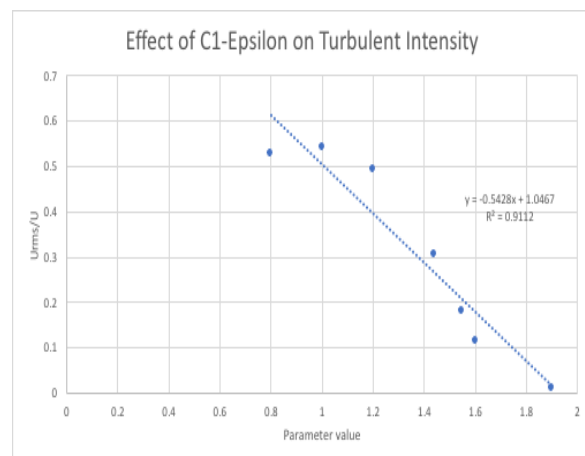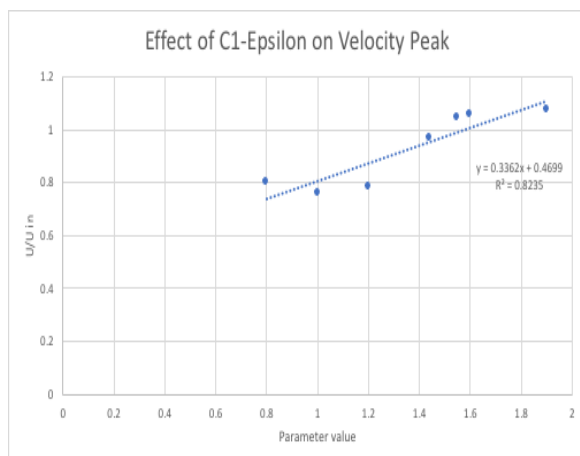
Figure 24: Effect of $C_{1,\epsilon}$ on Velocity Peak and Turbulence Intensity Graph

3rd Parameter: $C_{2,\epsilon}$
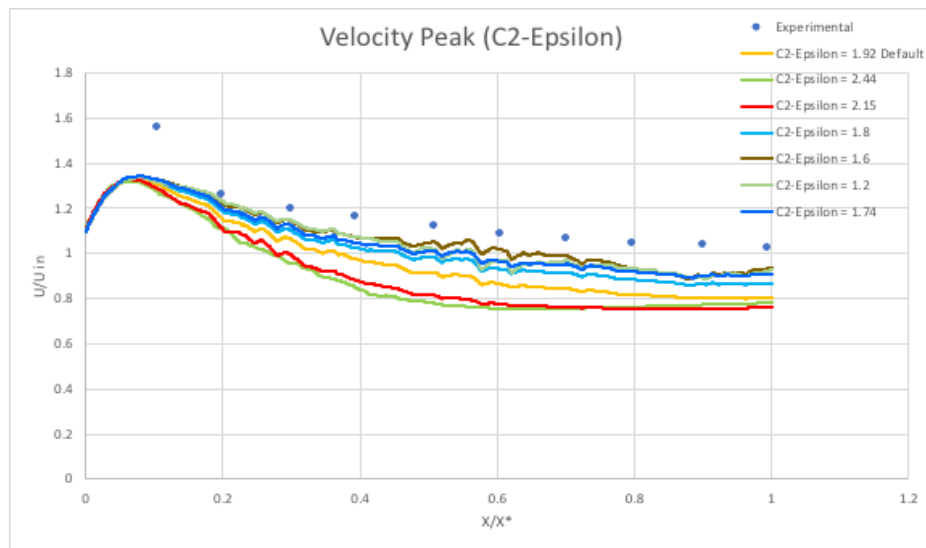
Figure 25: $C_{2,\epsilon}$ Velocity Peak graph
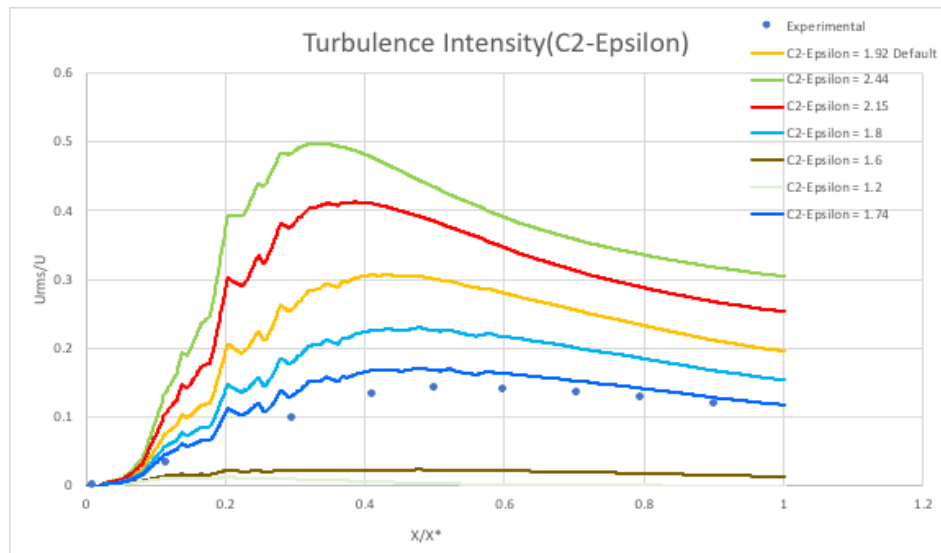
Figure 26: $C_{2,\epsilon}$ Turbulence Intensity graph
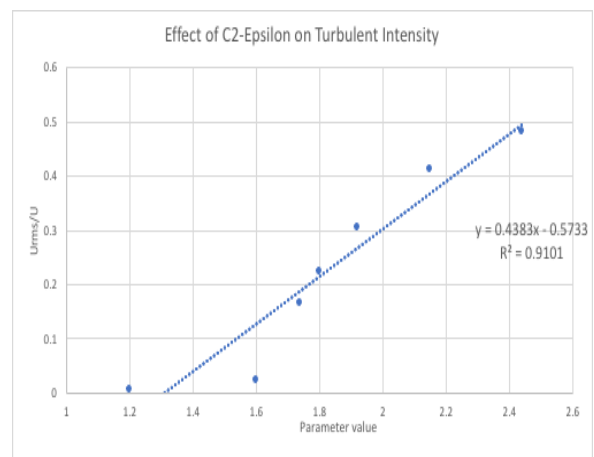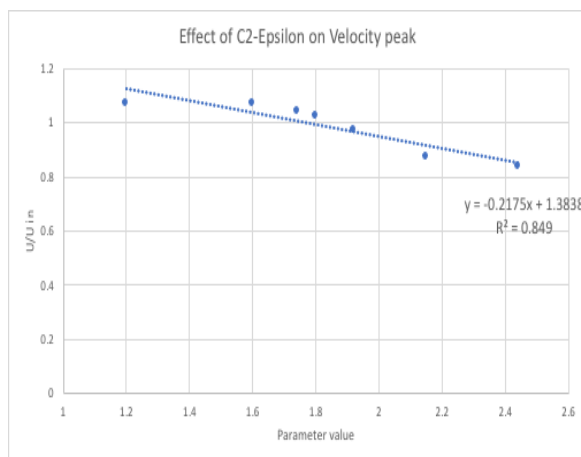
Figure 27: Effect of $C_{2,\epsilon}$ on Velocity Peak and Turbulence Intensity graph

4th Parameter: C_{1-PS}
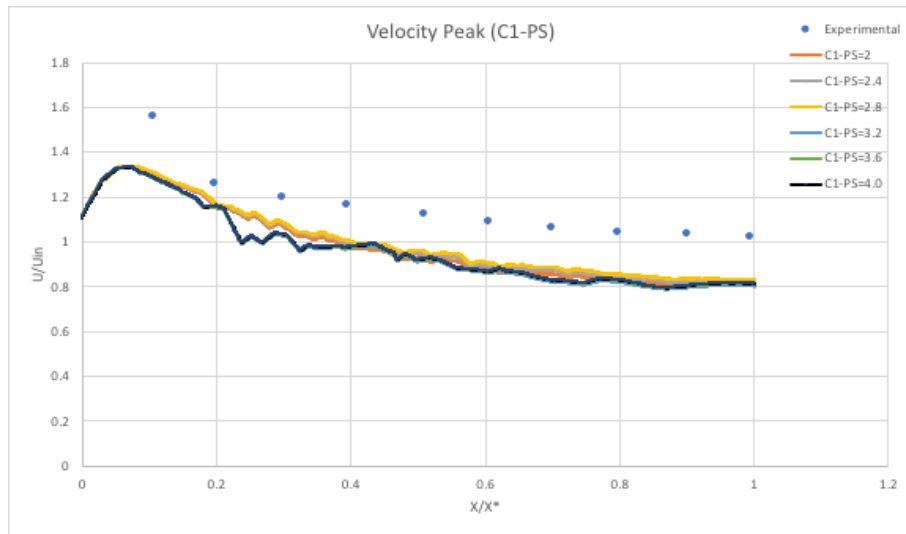
Figure 28: C_{1-PS} Velocity Peak graph
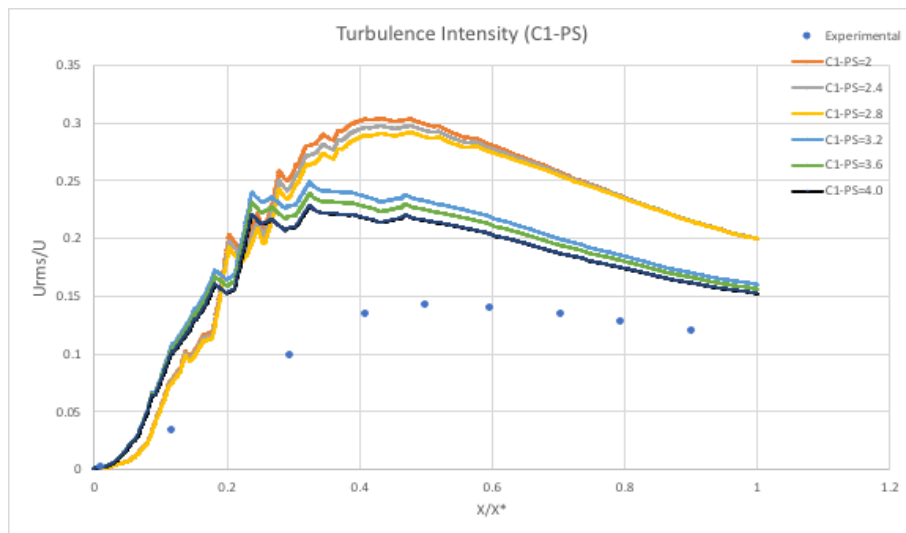
Figure 29: C_{1-PS} Turbulence Intensity graph
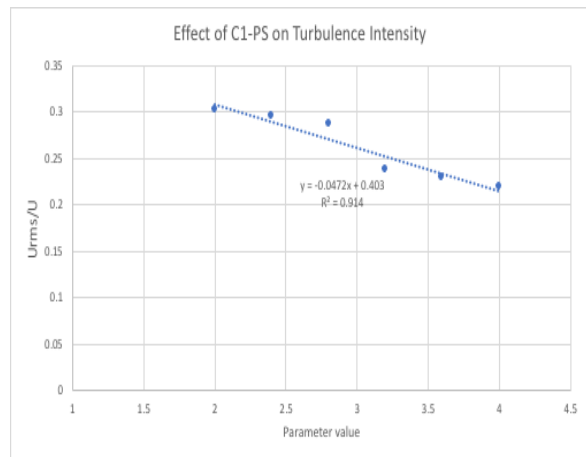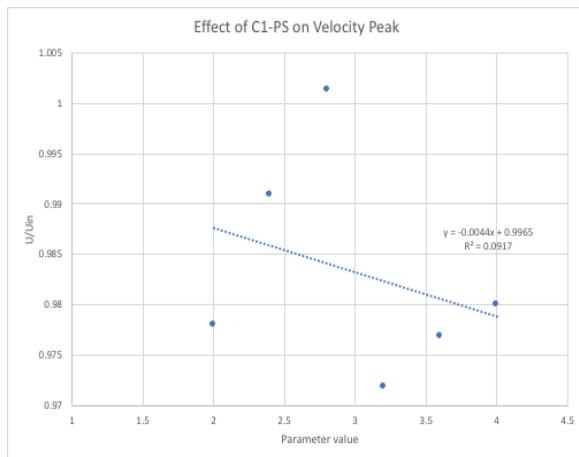
Figure 30: Effect of C_{1-PS} on Velocity Peak and Turbulence Intensity graph

5th Parameter: C_{2-PS}
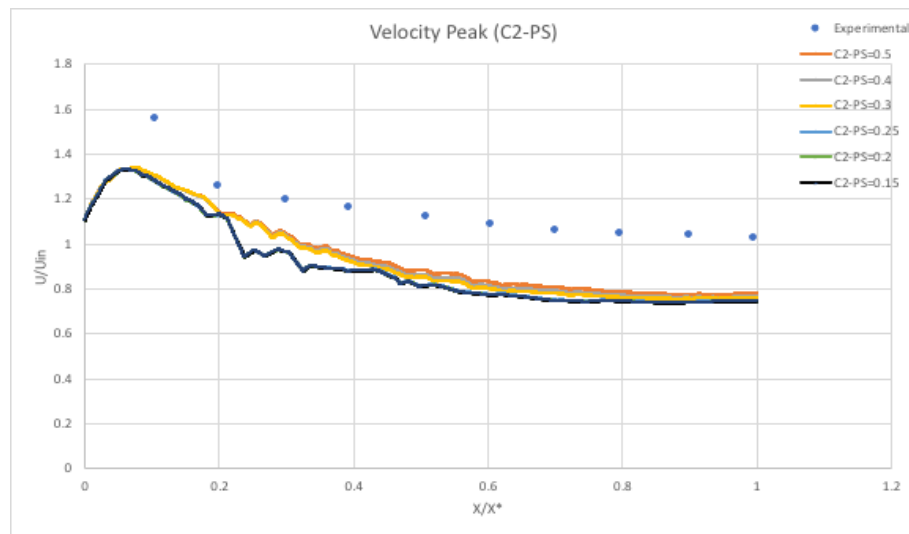
Figure 31: C_{2-PS} Velocity Peak graph
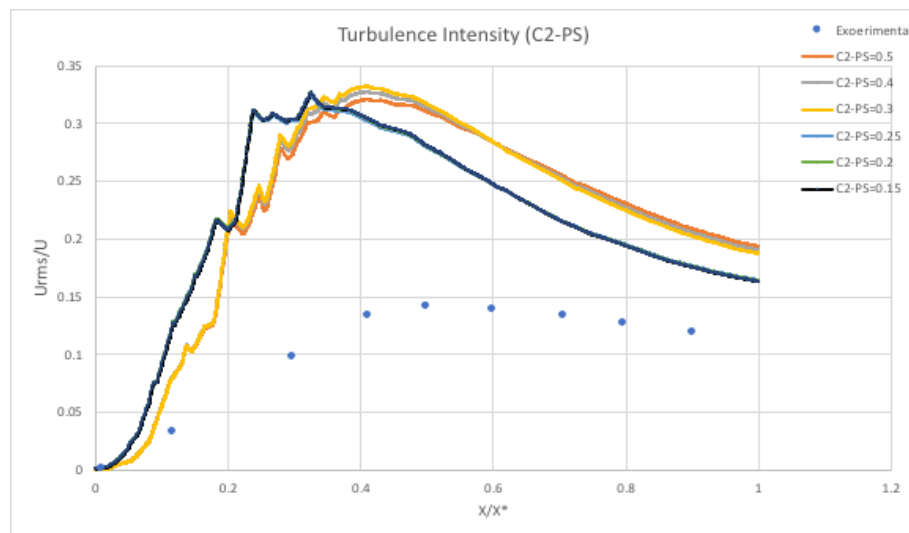
Figure 32: C_{2-PS} Turbulence Intensity graph
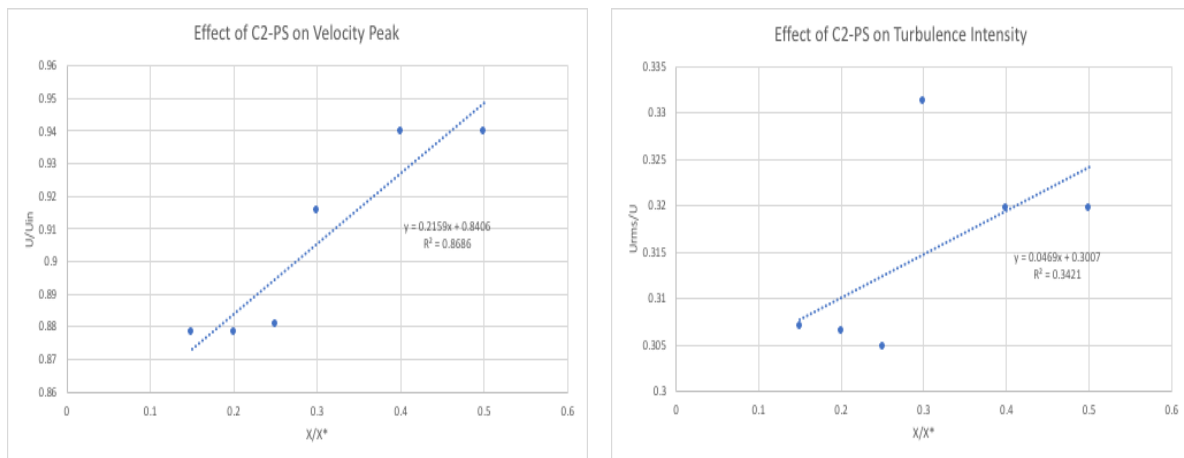
Figure 33: Effect of C_{2-PS} on Velocity Peak and Turbulence Intensity graph

6th Parameter: C'_{1-PS}
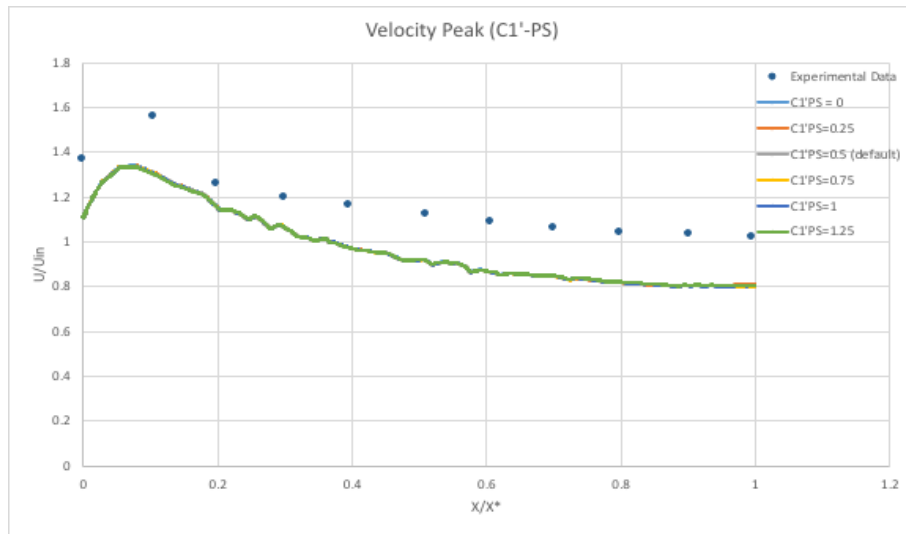
Figure 34: C'_{1-PS} Velocity Peak graph
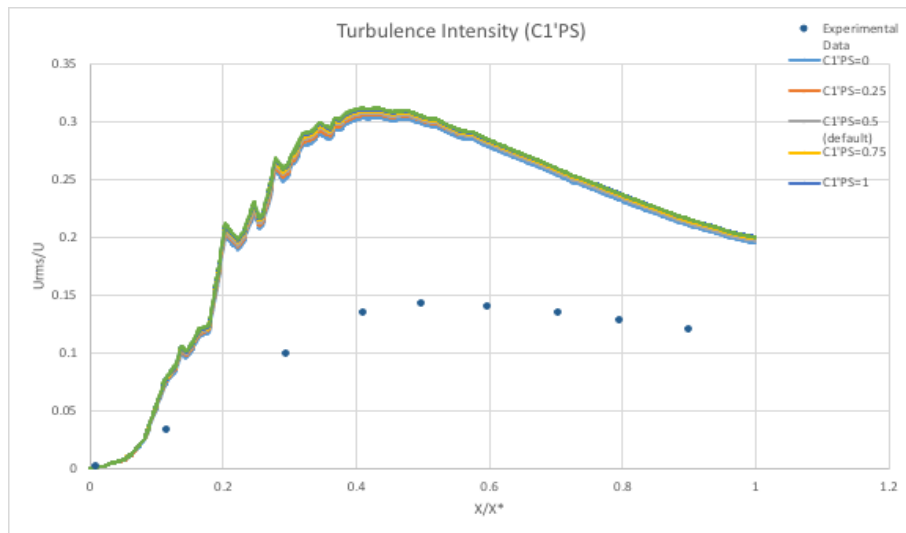
Figure 35: C'_{1-PS} Turbulence Intensity graph
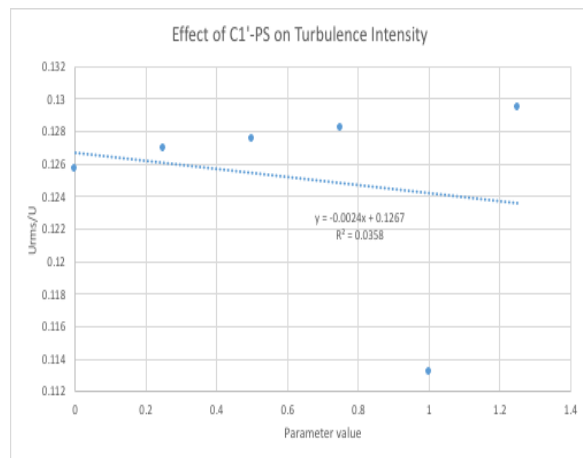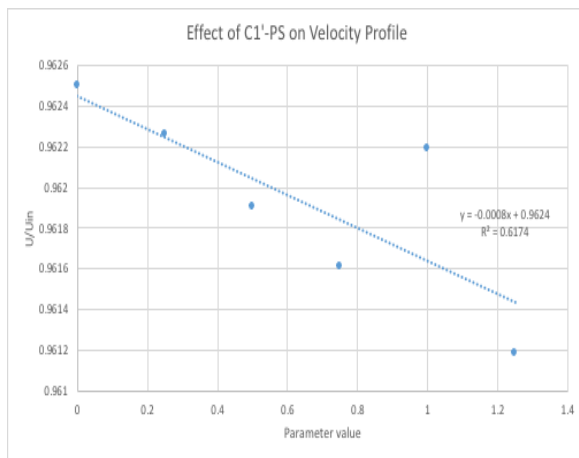
Figure 36: Effect of C'_{1-PS} on Velocity Peak and Turbulence Intensity graph

7th Parameter: C'_{2-PS}
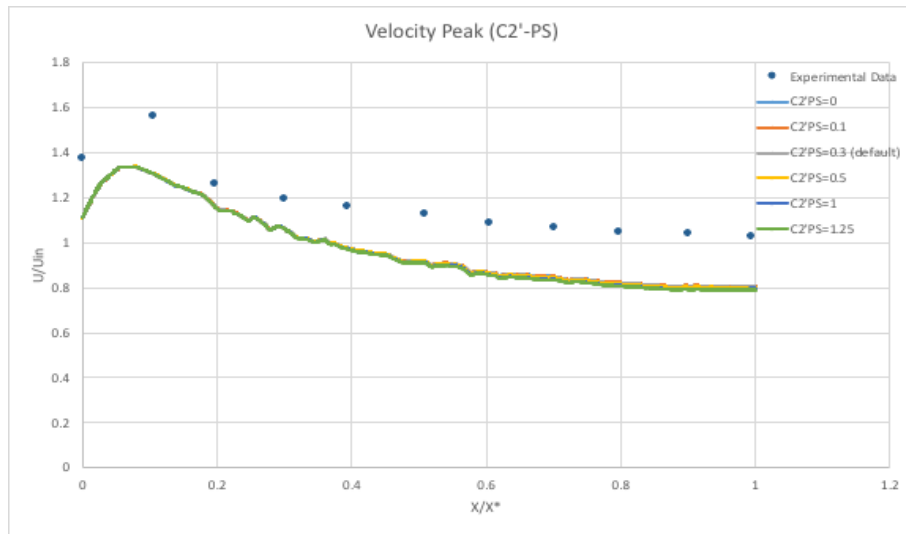
Figure 37: C'_{2-PS} Velocity Peak graph
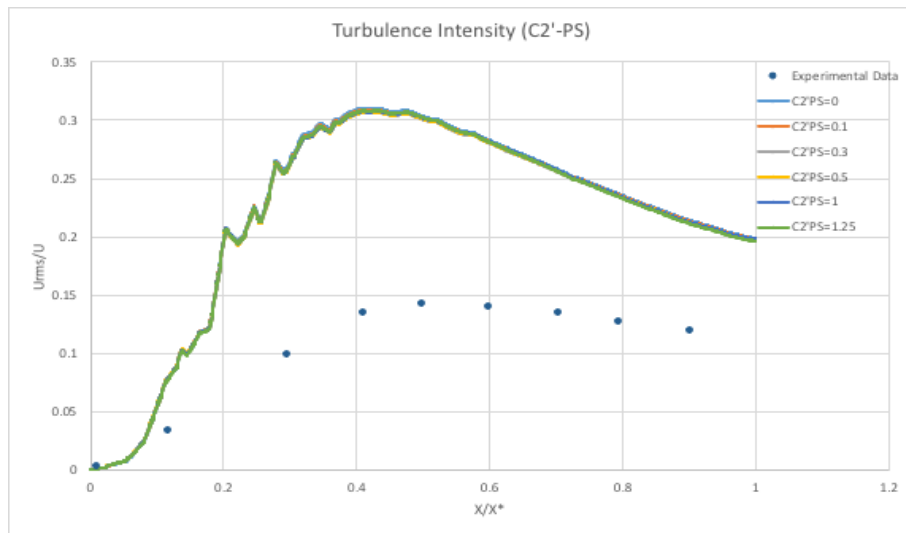
Figure 38: C'_{2-PS} Turbulence Intensity graph
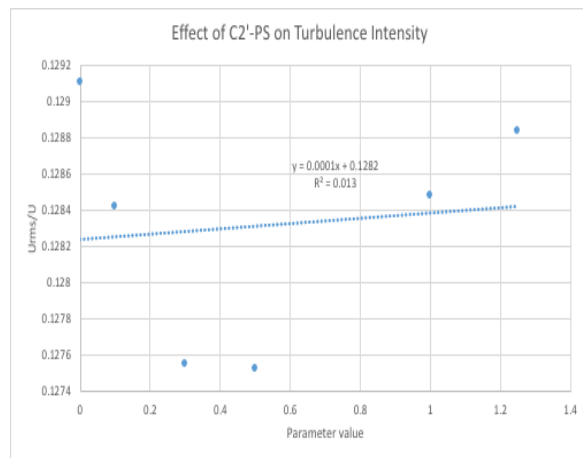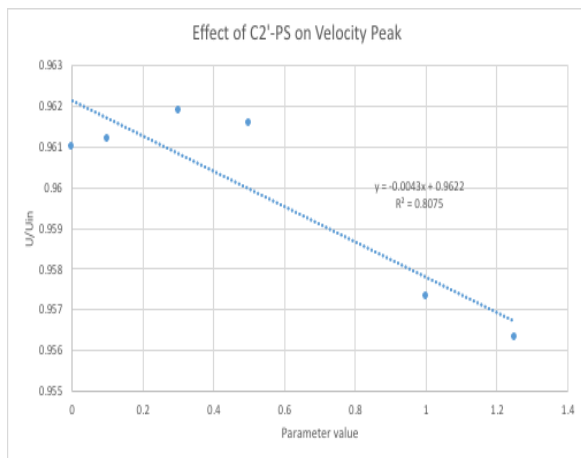
Figure 39: Effect of C'_{2-PS} on Velocity Peak and Turbulence Intensity graph

8th Parameter: Pr_{TKE}
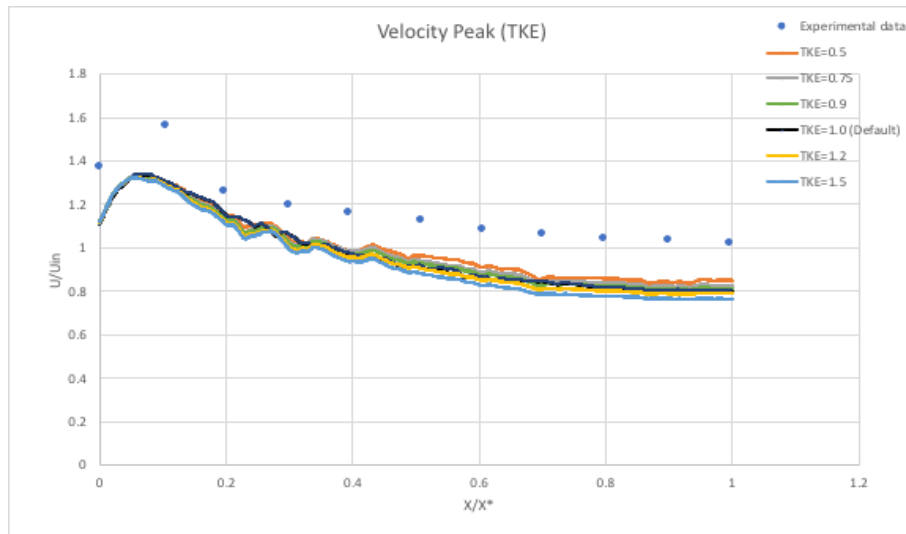
Figure 40: Pr_{TKE} Velocity Peak graph
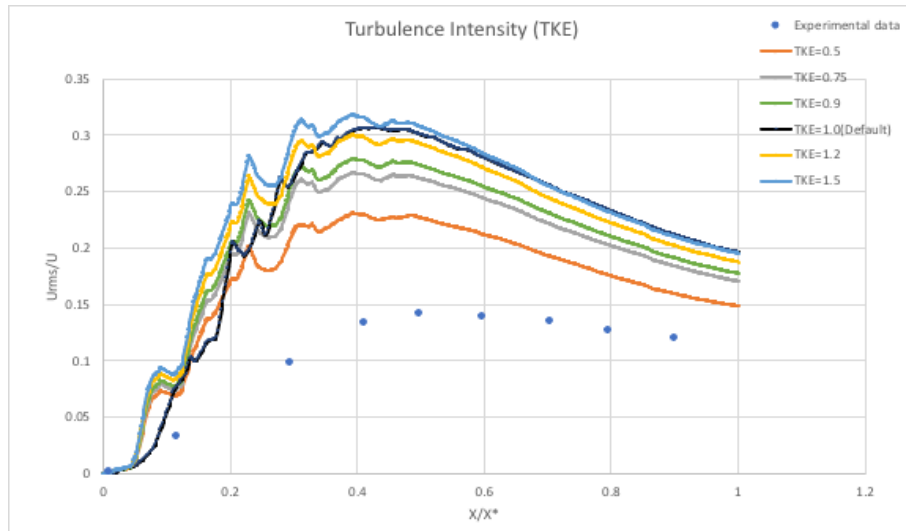
Figure 41: Pr_{TKE} Turbulence Intensity graph
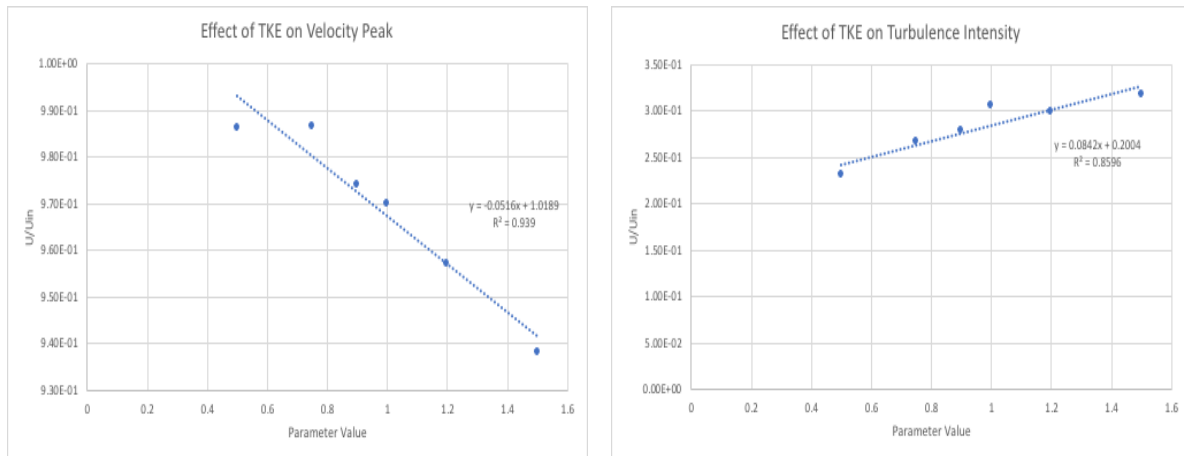
Figure 42: Effect of Pr_{TKE} on Velocity Peak and Turbulence Intensity graph

9th Parameter: Pr_{TDR}
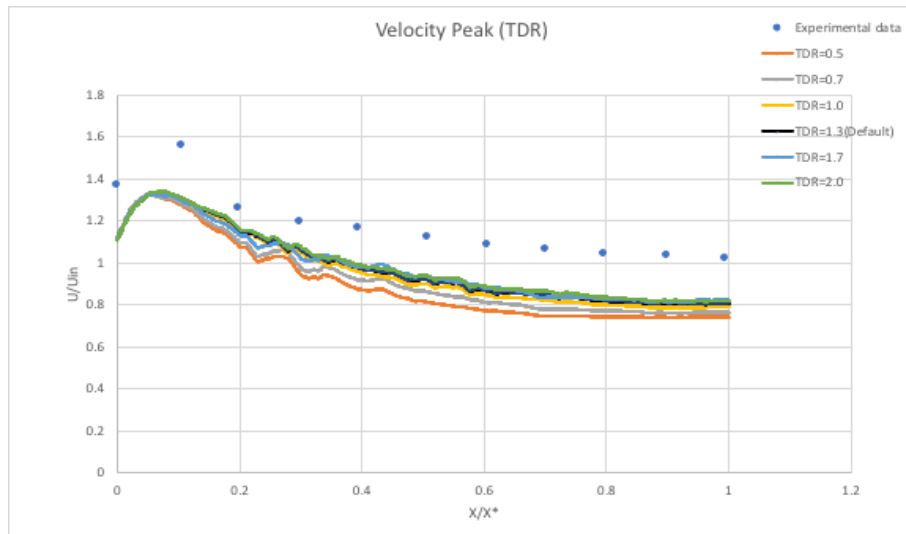
Figure 43: Pr_{TDR} Velocity Peak graph
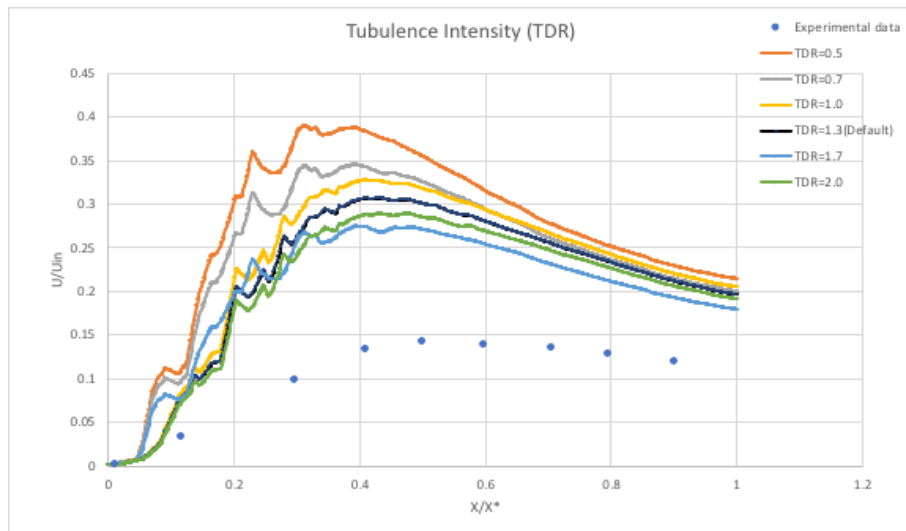
Figure 44: Pr_{TDR} Turbulence Intensity graph
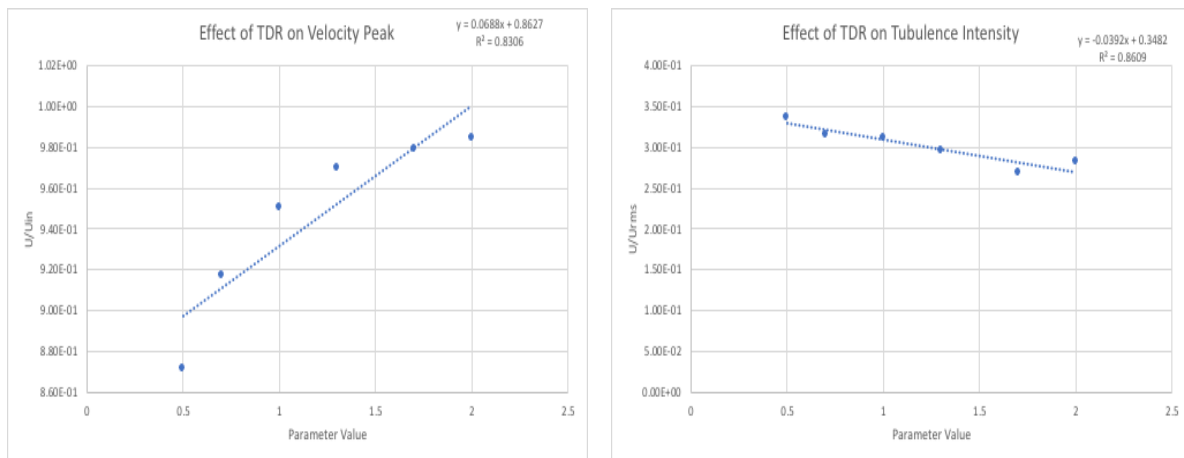
Figure 45: Effect of Pr_{TDR} on Velocity Peak and Turbulence Intensity graph

Ranking of Parameter changes
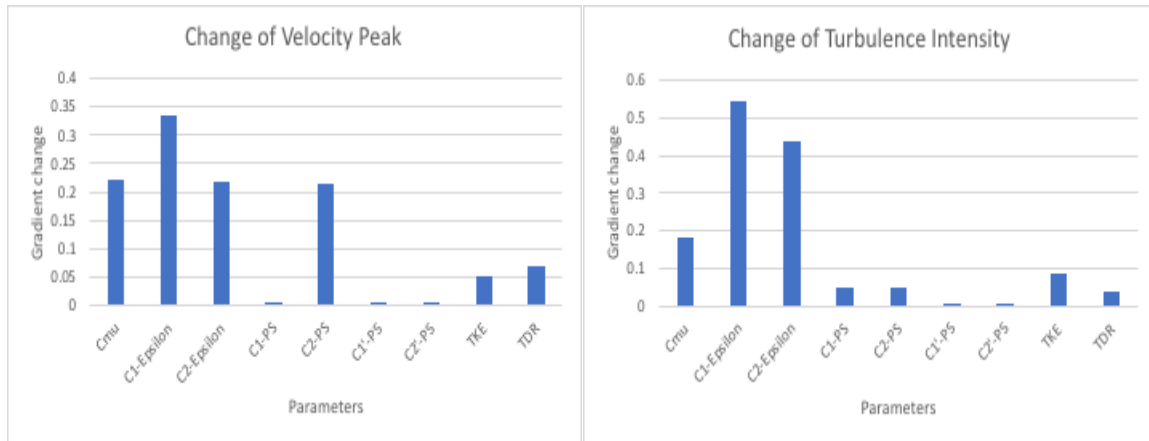
Figure 46: Ranking of each parameter change effect on the Velocity Peak and Turbulence Intensity

Tabulation of data

RSM Parameters	Velocity Peak (U/U_∞)		RSM Parameters	Velocity Peak (U/U_∞)	
	Gradient	Ranking		R^2	Ranking
$C_{1,\epsilon}$	0.3362	1	C_μ	0.9862	1
$C_{2,\epsilon}$	0.2175	2	Pr_{TKE}	0.9390	2
C_{2-PS}	0.2159	3	C_{2-PS}	0.8686	3
C_μ	0.2117	4	$C_{2,\epsilon}$	0.8490	4
Pr_{TKE}	0.0516	5	Pr_{TDR}	0.8306	5
Pr_{TDR}	0.0688	6	$C_{1,\epsilon}$	0.8235	6
C_{1-PS}	0.0044	7	C'_{2-PS}	0.8075	7
C'_{2-PS}	0.0043	8	C'_{1-PS}	0.6174	8
C'_{1-PS}	0.0008	9	C_{1-PS}	0.0917	9

Table 2: Degree of influence of RSM parameters on Velocity Peak

RSM Parameters	Turbulence Intensity Peak (U_{rms}/U)		RSM Parameters	Turbulence Intensity Peak (U_{rms}/U)	
	Gradient	Ranking		R^2	Ranking
$C_{1,\epsilon}$	0.5428	1	C_μ	0.9980	1
$C_{2,\epsilon}$	0.4383	2	$C_{1,\epsilon}$	0.9112	2
C_μ	0.1801	3	$C_{2,\epsilon}$	0.9101	3
Pr_{TKE}	0.0842	4	Pr_{TDR}	0.8609	4
C_{1-PS}	0.0472	5	Pr_{TKE}	0.8596	5
C_{2-PS}	0.0469	6	C_{2-PS}	0.3421	6
Pr_{TDR}	0.0392	7	C_{1-PS}	0.0914	7
C'_{1-PS}	0.0024	8	C'_{1-PS}	0.0358	8
C'_{2-PS}	0.0001	9	C'_{2-PS}	0.0130	9

Table 3: Degree of influence of RSM parameters on Turbulence Intensity

Parameter Tuning - $C_{1,\epsilon}$

Run	$C_{1,\epsilon}$	Velocity Peak			Turbulence Intensity		
		Experimental peak value	Simulated peak value	Percentage different (%)	Experimental peak value	Simulated peak value	Percentage different (%)
1	1.580	1.258352	1.213216	3.59	0.141701	0.143033	0.94
2	1.581	1.258352	1.205513	4.20	0.141701	0.141494	0.15
3	1.583	1.258352	1.214186	3.51	0.141701	0.139771	1.36
4	1.585	1.258352	1.210746	3.78	0.141701	0.139301	1.69
5	1.587	1.258352	1.211453	3.73	0.141701	0.133405	5.85

Table 4: Table of tuning of $C_{1,\epsilon}$
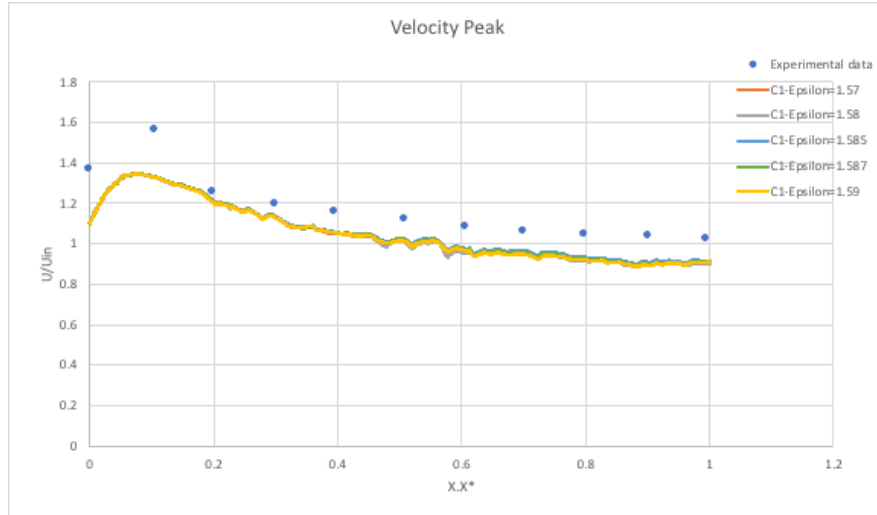
Figure 47: Tuning of $C_{1,\epsilon}$ on Velocity Peak
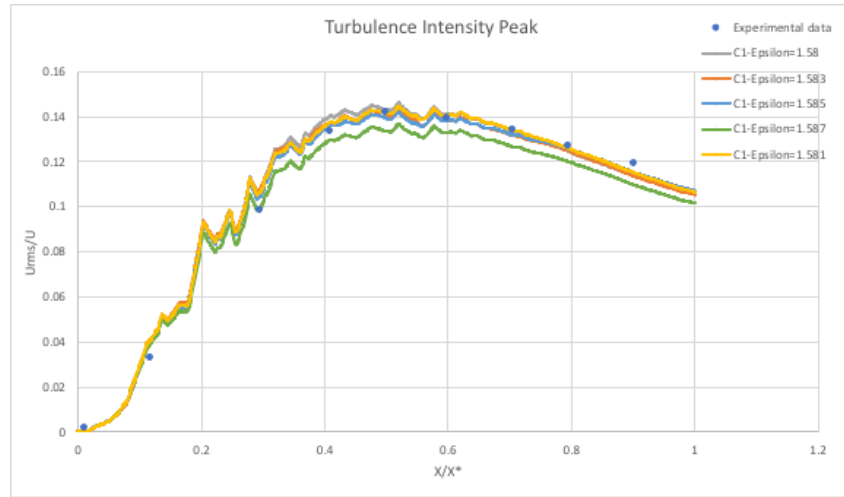
Figure 48: Tuning of $C_{1,\epsilon}$ on Turbulence Intensity

Parameter Tuning - $C_{2,\epsilon}$

Run	$C_{2,\epsilon}$	Velocity Peak			Turbulence Intensity		
		Experimental peak value	Simulated peak value	Percentage different (%)	Experimental peak value	Simulated peak value	Percentage different (%)
1	1.710	1.258352	1.203348	4.37	0.141701	0.131442	7.24
2	1.715	1.258352	1.216323	3.34	0.141701	0.134665	4.97
3	1.718	1.258352	1.202691	4.42	0.141701	0.141618	0.06
4	1.720	1.258352	1.203325	4.37	0.141701	0.142744	0.74
5	1.730	1.258352	1.205335	4.21	0.141701	0.155304	9.60

Table 5: Table of tuning of $C_{2,\epsilon}$
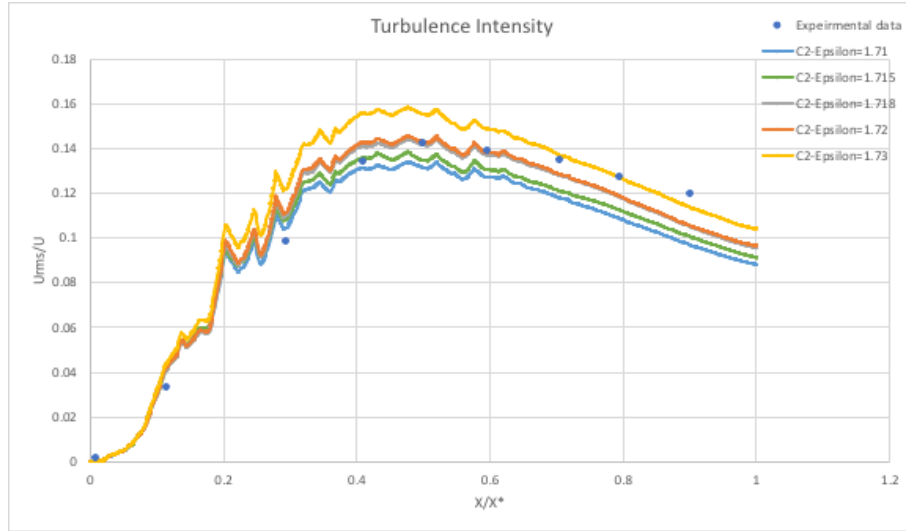
Figure 49: Tuning of $C_{2,\epsilon}$ on Turbulence Intensity
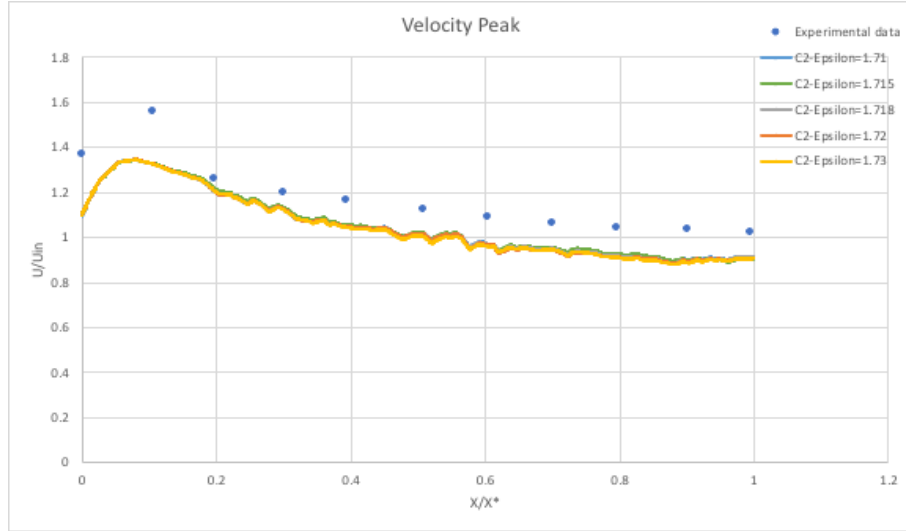
Figure 50: Tuning of $C_{2,\epsilon}$ on Velocity Peak

DISCUSSION

Turbulent viscosity parameter, C_μ

In a turbulent flow, the formation of eddies significantly controls the diffusion mechanism of the flow which leads to a term called turbulent viscosity, μ_t. The turbulent viscosity is a representation to estimate the net mixing rate of the inhomogeneous flow due to the eddies motion. In the transport equation of the Reynolds Stress Model (RSM), the turbulent viscosity is computed from the turbulent kinetic energy, k and the dissipation rate, ϵ which is similar to the $k - \epsilon$ mode:

$$\mu_t = \rho C_\mu \frac{k^2}{\epsilon}$$

(2)

where C_μ is the turbulent viscosity parameter which has a default value of 0.09 in ANSYS Fluent. The turbulent viscosity and turbulent viscosity parameter are indirectly related to the derivation of other terms in the Reynolds Stress Transport Equation as shown below:

Turbulent diffusion, $D_{T,ij}$

$$D_{T,ij} = \frac{\partial}{\partial x_k}\left(\frac{\mu_t}{\sigma_k}\frac{\partial \overline{u_i' u_j'}}{\partial x_k}\right) \tag{3}$$

Buoyancy production, G_{ij}

$$G_{ij} = \left(\overline{J_i U_j} + \overline{J_j U_i}\right) = -\beta\left(g_i \overline{u_j'\theta} + g_j \overline{U_i \theta}\right) \tag{4}$$

where

$$\overline{U_i \theta} = \frac{\mu_t}{Pr_t}\left(\frac{\partial T}{\partial X_i}\right) \tag{5}$$

Linear pressure strain, ϕ_{ij}

$$\phi_{ij} = \phi_{ij,1} + \phi_{ij,2} + \phi_{ij,w} \tag{6}$$

where

$$\phi_{ij,w} = C_i'\frac{\epsilon}{k}\left(\overline{u_k' u_m'}n_k n_m \delta_{ij} - \frac{3}{2}\overline{u_i' u_k'}n_j n_k - \frac{3}{2}\overline{u_j' u_k'}n_i n_k\right)\frac{C_l k^{3/2}}{\epsilon d} + C_2'\left(\phi_{km,2}n_k n_m \delta_{ij} - \frac{3}{2}\phi_{ik,2}n_j n_k - \frac{3}{2}\phi_{jk,2}n_i n_k\right)\frac{C_l k^{3/2}}{\epsilon d} \tag{7}$$

and

$$C_l = \frac{C_\mu^{3/4}}{\kappa} \tag{8}$$

Turbulence kinetic energy, k

$$\frac{\partial}{\partial t}(\rho k) + \frac{\partial}{\partial x_i}(\rho k u_i) = \frac{\partial}{\partial x_j}\left[\left(\mu + \frac{\mu_t}{\sigma_k}\right)\frac{\partial k}{\partial x_j}\right] + \frac{1}{2}(P_{ii} + G_{ii}) - \rho\epsilon(1 + 2M_t^2) + S_k \tag{9}$$

Dissipation rate, ϵ

$$\frac{\partial}{\partial t}(\rho\epsilon) + \frac{\partial}{\partial x_i}(\rho\epsilon u_i) = \frac{\partial}{\partial x_j}\left[\left(\mu + \frac{\mu_t}{\sigma_\epsilon}\right)\frac{\partial \epsilon}{\partial x_j}\right] C_{\epsilon 1}\frac{1}{2}[P_{ii} + C_{\epsilon 3}C_{ii}]\frac{\epsilon}{k} - C_{\epsilon 2}\rho\frac{\epsilon^2}{k} + S_\epsilon \tag{10}$$

Convective heat and mass transfer

$$\frac{\partial}{\partial t}(\rho E) + \frac{\partial}{\partial x_i}[u_i(\rho E + p)] = \frac{\partial}{\partial x_j}\left[\left(k + \frac{c_p \mu_t}{Pr_t}\right)\frac{\partial T}{\partial x_j} + u_i(\tau_{ij})_{eff}\right] + S_h \tag{11}$$

From Figure 19 and 20, it is observed that C_μ shows a predictable linear effect on the velocity profile as well as the turbulence intensity when inducing turbulence with RSM. This can be proven by having a high R^2 value (>0.98) for both streamwise velocity and turbulence intensity. As the C_μ value increases from the default value, the streamwise velocity along with the centreline increases and moves closer to the experimental results. For the turbulence intensity, it decreases towards the experimental findings as C_μ increases. Although C_μ is ranked at 4th for the influence on the streamwise velocity, it does not contribute to shifting the peak velocity. From figure 19, the peak velocity is at the same magnitude for all turbulent viscosity parameter change. The gradient in figure 21 is determined from the streamwise velocity at x/x* = 0.4, thus the influence of C_μ on the streamwise velocity only becomes obvious after the peak. For the influence of C_μ the turbulence intensity, it is ranked at 3rd, but the gradient is much smaller as compared to $C_{1,\epsilon}$ and $C_{2,\epsilon}$. Therefore, it can be concluded that C_μ is a non-dominant parameter for the RSM to best fit the experimental results.

Dissipation Parameters, $C_{1,\epsilon}$ and $C_{2,\epsilon}$

Both $C_{1,\epsilon}$ and $C_{2,\epsilon}$ are the constants used in the transport equation of RSM for the dissipation rate, ϵ which have the default values of 1.44 and 1.92 respectively. The dissipation rate is associated with the turbulence kinetic

energy where the kinetic energy cascades down from large to small eddies by the interactional forces between the eddies. Thus, the dissipation rate is a measure to determine the amount of energy dissipated by the eddies into heat due to viscous forces in the turbulent flow. In ANSYS, the dissipation rate is computed with a model transport equation similar to that used in the standard $k - \epsilon$ model, as shown in equation (10). From Table 2 and 3, in term of the gradient ranking, $C_{1,\epsilon}$ and $C_{2,\epsilon}$ are ranked at 1st and 2nd respectively for both the influence of parameters on the velocity profile and turbulence intensity. The gradient magnitude is much larger as compared to the other parameters. This implies that $C_{1,\epsilon}$ and $C_{2,\epsilon}$ are the dominant parameters in inducing turbulence using RSM. Figure 23 and 26, it can be observed that the change in $C_{1,\epsilon}$ and $C_{2,\epsilon}$ significantly shifting the peak of the turbulence intensity. From the research, as $C_{1,\epsilon}$ increases or $C_{2,\epsilon}$ decreases from the default value, the curve of the turbulence intensity moves more towards the experimental results. Since the R^2 value of the trendline is quite high for both $C_{1,\epsilon}$ and $C_{2,\epsilon}$ parameter change, it can be estimated for the simulated turbulence intensity curve to best fit the experimental curve, the optimum $C_{1,\epsilon}$ value is around 1.581 with a percentage error of 0.15% whereas for $C_{2,\epsilon}$ is around 1.718 with a percentage error of 0.06 as presented in Table 4. However, both parameters do not play a role in optimising the velocity peak location.

The reason that the dissipation parameters have such a dominant effect in modelling the turbulence is due to the presence of the single square grid. The default values of $C_{1,\epsilon} = 1.44$ and $C_{2,\epsilon} = 1.92$ are determined from experiments with air and water for fundamental turbulent shear flows including homogeneous shear flows and decaying isotropic grid turbulence. They have been found to work fairly well for a wide range of wall-bounded and free shear flows. However, the single square grid acts as a blockage to distort the fluid flow. The fluid experiences a sudden acceleration when flowing through the grid but there is an intensive formation of wakes due to the vortex shedding after passing through the grid. The generated wakes at the downstream causing the flow to become highly inhomogeneous and anisotropic. Furthermore, the interaction of wakes with the fluid creates forced shearing which facilitates the formation of large turbulence eddies. This significantly alters the dissipation rate of the fluid flow kinetic energy therefore the tuning in the dissipation parameters $C_{1,\epsilon}$ and $C_{2,\epsilon}$ is important for the simulation of the induced turbulence by the single square grid using RSM.

Linear pressure strain parameters, C_{1-PS}, C_{2-PS}, C'_{1-PS} and C'_{2-PS}

The pressure strain term in the RSM transport equation is modelled according to the proposals by Gibson and Launder, Fu et al. and Launder as expressed in equation (6). The linear pressure strain is composed by the slow pressure-strain term, rapid pressure-strain term and the wall reflection term. C_{1-PS} and C_{2-PS} are related to the slow pressure-strain term and rapid pressure-strain term respectively. ANSYS Fluent uses $C_{1-PS} = 1.8$ and $C_{2-PS} = 0.6$ as default values which is suitable for flows with relatively high Reynolds Number. The remaining 2 parameters C'_{1-PS} and C'_{2-PS} are related to the equation of wall reflection term and are responsible for redistributing stresses near the wall. The default values from ANSYS are $C'_{1-PS} = 0.5$ and $C'_{2-PS} = 0.3$ which is again suitable for most flows at high Reynolds number. Based on the velocity profiles generated by all four linear pressure strain parameters, it can be concluded that all the linear pressure strain parameters do not contribute to shifting the velocity peak location. Furthermore, it is found that both parameter changes for C'_{1-PS} and C'_{2-PS} do not have a significant influence on the turbulence intensity as well. This is expected as the data collected are along the centreline which is relatively far from the wall thus the effect of wall reflection term in the linear pressure strain is negligible.

On the other hand, it can be observed that C_{1-PS} has an obvious influence on the turbulence intensity among the other pressure strain parameters. However, it requires a large increase in the parameter value to make the turbulence intensity curve moves closer to the experimental results. This might be impractical as the illogical large value might disobey the nature of the governing equation. This can also be explained by almost 10 times lower gradient magnitude (0.0472) of C_{1-PS} as compared to the dominant parameters $C_{1,\epsilon}$ and $C_{2,\epsilon}$. Henceforth, it can be concluded that the influence of these four linear pressure strain parameters are insignificant in the turbulence modelling.

Prandtl number parameters, Pr_{TKE} and Pr_{TDR}

The Turbulent Kinetic Energy (TKE) Prandtl Number defines the ratio of the momentum diffusivity to the diffusivity of turbulence kinetic energy via turbulent transport whereas the Turbulent Dissipation Rate (TDR) Prandtl Number defines the ratio of the momentum diffusivity to the diffusivity of turbulence dissipation via turbulent transport. They are used to compute the turbulence kinetic energy and dissipation rate as expressed in

equation (9) and (10) respectively in term of σ_k and σ_ϵ respectively. From the graphical results from figure 40,41,43 and 44, it is observed that the changes in parameter value of both Pr_{TKE} and Pr_{TDR} do not bring any effects on the velocity profile of the induced turbulence. This can be confirmed by the gradient magnitude of these parameters which is much lower than the dominant parameters. Besides that, as Pr_{TKE} decreases whereas Pr_{TDR} increases from their default values, the turbulence intensity curve shifts towards the experimental results. This agrees with the theory since both Pr_{TKE} and Pr_{TDR} contribute to the turbulent kinetic energy and dissipation rate which have a remarkable influence on the turbulence intensity. However, it required a large deviation from the default value to achieve the best fit which might contradict with the nature of the governing equation. Generally, the Prandtl number is accounting for the anisotropic production in the near-wall region [16], but in this simulation, the data taken are along the centreline of the channel with is away from the walls. Thus, both Pr_{TKE} and Pr_{TDR} are considered to have insignificant effect if compared with $C_{1,\epsilon}$ and $C_{2,\epsilon}$.

Future improvement suggestions

Due to the limitations of the computer power limit and the student version of ANSYS Fluent, the minimum mesh size can be achieved is only 18mm with a total of 490,000 elements. To improve the accuracy, a smaller mesh size must be applied to the model so that a more precise change between adjacent elements can be captured to give a better simulation result. Apart from that, since the RSM equations are highly non-linear and are closely related, manipulate the parameters in pairs or three by three can produce a more accurate turbulence modelling due to the combined effects from multiple parameters. Another improvement is to link ANSYS Fluent with MATLAB because MATLAB has the advance built-in functions for plotting and creating trendline which helps in analysing and tuning process.

CONCLUSION

The experiment was successful in identifying the parameters which have the most influence on the Reynold Stress Equation. Both velocity charts and turbulence intensity charts are most affected by the C1-Epsilon and C2-Epsilon parameter. However, more research is needed to be done until the velocity and turbulence charts are fully matched with the one found in literature. Moreover, more powerful hardware will be required to run finer meshes and additional iterations during simulations. This more powerful hardware will not only improve the accuracy of the results but also allow simulations to be completed faster. Additionally, more than one parameter has yet to be varied and its affected observed, this should be a priority in future research.

REFERENCES

[1]   Q. Nguyen, D. Papavassiliou, "Quality measures of mixing in turbulent flow and effects of molecular diffusivity", Fluids 3(53) (2018).

[2]   I.Paul, G.Papadakis, J.C.Vassilicos, "Genesis and evolution of velocity gradients in nearfield spatially developing turbulence" in JOURNAL OF FLUID MECHANICS,volume 815,pp 295-332

[3]   Y. Zhou, K. Nagata, Y. Sakai, H. Suzuki, Y. Ito, O. Terashima, T. Hayase, Development of turbulence behind single square grid, Physics of Fluids 26, 045102

[4]   Mazellier, J. C. Vassilicos, Turbulence without Richardson-Kolmogorov cascade, Phys. Fluids 22, 075101

[5]   Pelin Ilker, Mehmet Sorgun, " Performance of turbulence models for single phase and liquid-solid slurry flows in pressurized pipe systems" in Ocean Engineering,volume 214

[6]   Turk, Jodi, Zhang, Wei, & Omilion, Alexis. (2018). Turbulence Enhancement by Fractal Square Grids: Effects of Multiple Fractal Scales. Fluids., 3(2).

[7]   Thomas Sponfeldner,Nikolaos Soulopoulos,Frank Beyrau,Yannis Hardalupas,Alex M.K.P. Taylor, J.Christos Vassilicos, "The structure of turbulent flames in fractal-and regular-grid-generated turbulence" in Combustion and Flame, volume 162,pp 3379-3393

[8]   L. Tian, G. Ahmadi, Particle deposition in turbulent duct flows-comparisons of different model predictions, Journal of Aerosol Science 38 (2007),pp 377-397

[9]   S. K. Lele, Compact finite difference schemes with spectral-like resolution, Journal of Computational Physics 103 (1992), pp 16-42

[10]   K. Nagata, H. Suzuki, Y. Sakai, T. Hayase, Direct numerical simulation of turbulence with scalar transfer around complex geometries using the immersed boundary method and fully conservative higher-order finite-difference schemes, IntechOpen (2010),pp 39-62

[11]   H. Suzuki, K. Nagata, Y. Sakai, T. Hayase, Y. Hasegawa, T. Ushijima, An attempt to improve accuracy of higher-order statistics and spectra in direct numerical simulation of incompressible wall turbulence by using the compact schemes for viscous terms, Int. Journal for Numerical Methods in Fluids 73 (2013), pp 509.

[12]   M. M. Gibson, B. E. Launder, Ground Effects on Pressure Fluctuations in the Atmospheric Boundary Layer, Journal Fluid Mech., (1978) 491-511.

[13]   S. Fu, B. E. Launder, M. A. Leschziner, Modeling Strongly Swirling Recirculating Jet Flow with Reynolds-Stress Transport Closures. In Sixth Symposium on Turbulent Shear Flows, Toulouse, France (1987)

[14]   B. E. Launder, Second-Moment Closure and Its Use in Modeling Turbulent Industrial Flows, International Journal for Numerical Methods in Fluids (1989) 963-985.

[15]   B. E. Launder, Second-Moment Closure: Present... and Future?, Int. Journal of Heat and Fluid Flow 10 (1989) 282-300.

[16]   Md Mizanur Rahman et al, Impact of Prandtl numbers on turbulence modelling, J. Phys.: Conf. Ser. 1324 012060, 2019

APPENDICES

RISK ASSESSMENT

HIRARC FORM				
Company:	Monash University Malaysia	Conducted by:	Mr. Lim Wei Chun, Mr. Adriel Sebastian Joseph, Mr. Toh Wu Peng, Mr. Yong Wen Jun, Mr. Ooi Jia Yong, Mr. Abdulhadi Faiz Arnaut (students) 11 September 2019 to 30 October 2019	
Process / Location:	Simulation / Home			
Approved by: (Name, designation)	Dr. Foo Ji Jin (supervisor)			
Date:	11 September 2020	Review Date:	1.	2.

1. Hazard Identification			2.Risk Analysis				3. Risk Control	
No.	Work Activity	Hazard	Which can cause/effect	Existing Risk Control	Likelihood	Severity	Risk	Recommended control measures	PIC(Due date/status)
1	Long hours of staring the process of numerical simulation	Excessive eye exposure to computer screen	Fatigue and eye strain	Ensure a good distance between the screen and user	4	3	12 (Medium)	Users are recommended to take a break after prolonged user	30 October 2020 / In progress
2	Long hours of sitting in front of the computer	Poor body posture of sitting	Muscle pain around the back and neck	Stretch, stand and walk around after pro-longed usage	3	3	9(Medium)	Use a ergonomic chair to correct the sitting posture and practice a good sitting posture	30 October 2020 / In progress
3	Moving around at workplace	Cables are scattered around on the floor	Users may trip over the messy computer cables	User needs to alert themselves about the surroundings	2	4	8(Medium)	Practice good cable management	30 October 2020 / In progress

4	Doing the documentation through computer	Computer crashes or power failure	Loss of the result and documentation for the report	User need to save their working file every 15 minutes	2	5	10(Medium)	Auto backup the files into the cloud drive to ensure no data loss	30 October 2020 / In progress
5	Group meeting	Conflict between the team members	Cohesion between group members affected and lower productivity	Practice good communication habit among each other	4	4	16(High)	Resolve any issues at the beginning stage to ensure all team members have the same objective and expectation when doing the research	30 October 2020 / In progress
6	Performing numerical simulation through computer	Overload the CPU usage which leads to CPU overheat	Loss of simulation data	Avoid running the numerical simulation over 8 hours in one day	3	5	15(High)	Reduce the usage of CPU or perform the numerical simulation on a powerful CPU core	30 October 2020 / In progress
7	Doing the research study	Encounter stress about the research project	Lost of confidence and resist to do the research	Gantt chart is applied to ensure the research project can be completed on time	4	4	16(High)	Extend the deadline of the submission of the research project and have weekly face to face guidance from the lecturer	30 October 2020 / In progress